Vernet, N.; Ruiz, E.; Advani, S.; Alms, JB.; Aubert, M.; Barburski, M.; Barari, B.... (2014). Experimental determination of the permeability of engineering textiles: Benchmark II. Composites Part A: Applied Science and Manufacturing. 61:172-184. doi:10.1016/j.compositesa.2014.02.010.

Experimental determination of the permeability of textiles:

Benchmark II

S. Advani [a], M. Aubert [b], M. Barburski[i] J.M. Beraud [b], D.C. Berg [c], A. Endruweit [d], P. Ermanni [e], J. Garcia [f], A. George [g], C. Hahn [h], S.V. Lomov [i], A. Long [d], V. Michaud [j], H. Perrin [k], K. Pillai [l], E. Rodriguez [m], E. Ruiz [n*], F. Trochu [n], N. Vernet [n], M. Weitgrefe [o], G. Ziegman [c]

[a] *Department of Mechanical Engineering, University of Delaware, USA*
[b] *Hexcel Reinforcements, Les aveniers, France*
[c] *Institut für Polymerwerkstoffe und Kunststofftechnik, Technische Universität Clausthal, Germany*
[d] *Division of Materials, Mechanics and Structures, University of Nottingham, UK*
[e] *Centre of Structure Technologies, Eidgenössische Technische Hochschule Zürich, Switzerland*
[f] *Instituto de Technologia de Materiales, Universitat Politècnica de València, Spain*
[g] *Swerea SICOMP, Sweden*
[h] *Institue for Carbon Composites, Technische Universität Munich, Germany*
[i] *Department of Metallurgy and Materials Engineering, KU Leuven, Belgium*
[j] *Laboratoire de Technologie des Composites et Polymères, École Polytechnique Fédérale de Lausanne, Switzerland*
[k] *Centre technique international de mise en oeuvre de matériaux composites, PPE, France*
[l] *Mechanical Engineering Department, University of Wisconsin, USA*
[m] *Institute of Material Science and Technology, National University of Mar del Plata, Argentina*
[n] *Chair on Composites of High Performance, École polytechnique de Montréal, Canada*
[o] *Airbus, Germany*

[*] Corresponding author: *edu.ruiz@polymtl.ca*

Abstract:

In this second international permeability benchmark, the in-plane permeability values of a carbon fabric were determined by 12 participants worldwide. One other participant also investigated the deformation of this fabric. The aim of this work was to obtain comparable results in order to make a step towards standardization of permeability measurements of fibrous reinforcements. The procedures used by most participants were according to the guidelines defined for this exercise after the first benchmark. Unidirectional injections in three in-plane directions of the fabric were conducted to determine the unsaturated in-plane permeability tensor. Parameters such as fiber volume fraction, injection pressure and fluid viscosity have been fixed in order to minimize sources of scatter. The comparison of the results from each participant was encouraging. The scatter between data obtained while respecting the test guidelines was close to the scatter of the setups themselves. A slightly

higher dispersion was observed when some parameters differed from the recommendations. Overall, a good correlation is observed between all the results of this exercise.

Keywords: fabrics/textiles, process monitoring, resin flow, permeability

1. Introduction

Liquid Composite Molding (LCM) processes are increasingly used in the automotive, and aeronautic industries. Five common steps in LCM are necessary to manufacture a composite part. Firstly, the fibrous reinforcement is preformed to the geometrical shape of the final part. Then, the preform is placed in the mold cavity. A flexible or rigid top is used to close the mold in order to inject the polymeric resin in the next step. Once the mold is completely filled, the resin is cured. Finally, the component can be demolded.

The filling of complex-shaped molds is a critical step. Indeed, dry zones may appear if specifications like positions of injection and vent gates, injection pressure and clamping force are not well defined. RTM simulation softwares such as PAM-RTM [1], LIMS [2] and Polyworx [3] allow to obtain filling times, flow front shapes, pressure and velocity fields of a complete manufacturing process in order to optimize mold designs and injection parameters. However, a complete characterization of the material properties influencing the impregnation of the fibrous reinforcement is necessary to run such simulations.

The permeability of fibrous reinforcement is one of the key parameters governing the mold filling. It corresponds to the ease of fluid flow through a porous media. This property was first proposed by Darcy in 1856. Based on the observation of water flowing through a vertical column of sand, he derived an empirical formula now known as Darcy's law [4]:

$$v = -\left(\frac{K}{\mu}\right) \cdot \nabla P \tag{1}$$

where v, μ, ∇P and K are respectively the Darcy velocity, the dynamic viscosity, the pressure gradient and the permeability. For porous media such as fibrous reinforcements, the permeability is anisotropic. Thus the second order tensor describing this property can be written as:

$$K = \begin{bmatrix} K_{xx} & K_{xy} & K_{xz} \\ K_{yx} & K_{yy} & K_{yz} \\ K_{zx} & K_{zy} & K_{zz} \end{bmatrix} \quad (2)$$

This tensor can be diagonalized to obtain the three principal permeability values of a fibrous reinforcement: K_1 and K_2 in the plane and K_3 through the thickness of the fiber bed. The in-plane flowing pattern is thus an ellipse oriented at an angle β corresponding to the angle between the warp direction and the principal flow direction. In-plane principal permeability values are of particular interest because most of composite manufacture is performed by injecting resin in the plane of the fibrous reinforcement.

A wide variety of methods exist to determine the in-plane permeability of a fibrous reinforcement. Firstly, it is possible to predict the permeability via models. Kozeny and Carman [5] or Gebart [6] have developed equations taking into account fiber geometrical parameters and the fiber volume fraction to calculate the permeability of a single scale porous medium. This kind of model is still used to approximate the permeability of a fiber tow. However, they are not well adapted to determine the permeability of dual scale porous media such as fabric. Thus, more complex analytical models, as for example Lundström [7] or Papathanasiou [8], have been created considering the fibrous reinforcement as a medium composed of fiber tows. Thus, the flow was divided in two components: the flow in the tows (capillary) and the flow between the tows (viscous). Numerical simulations have also been developed to calculate the permeability of a fibrous reinforcement. Various techniques have been explored: lattice Boltzmann method [9], finite differences calculation [10, 11], and finite element method [12]. However, to validate all these models, experimental data of permeability are necessary. Moreover, permeability measurement is the only way to obtain accurate values.

Numerous experimental techniques have been developed, as summarized in [13]. Two of them are commonly used to determine K_1 and K_2: unidirectional [14, 15] and radial techniques [16, 17]. Both methods show advantages and drawbacks. The former method has a higher repeatability thanks to an easier tracking of the straight unidirectional flow front, and can be used to determine both unsaturated permeability by following the flow front and saturated permeability, after the flow has filled the entire preform. However, the radial method permits to determine the permeability ellipse with only one experiment. In addition, the possible race-tracking observed in a unidirectional measurement [18] is avoided here.

The lack of standardization of permeability measurements impedes researchers from comparing permeability obtained from different setups. Parnas et al. [19] and Lundström et al. [20] have respectively initiated the creation of a permeability database and a small-scale benchmark. Their efforts were important, but the implication of a larger part of the composite world is necessary to take a step towards standardization. An initial international permeability benchmark exercise [21], initiated by ONERA (Office National d'Étude et de Recherche Aérospotiales, France) and Katholieke Universiteit Leuven, was conductd for this purpose. The aim was to get an overview of the methods, practical uses and range of results of different participants worldwide. The permeability data of twenty institutions from twelve countries on two different fabrics were compiled and compared. The main finding of this study was a significant scatter of up to one order of magnitude between all participants for both reinforcements tested. The explanation then was that human factors such as skilled and experienced personnel, preparation of specimens or evaluation of raw data were principally responsible for this scatter. In that work, it was suggested that another benchmark based on a common procedure and more controlled experimental conditions has to be performed in order to allow a more quantitative comparison of the results.

For this purpose, a guideline document [22] has been written in a collaborative effort among the participants of this first exercise. In these guidelines, test conditions for unidirectional unsaturated permeability measurements are defined. Based on them and the common desire of researchers to standardize the determination of permeability, a second benchmark was agreed with the support of Hexcel Fabrics. A total of twelve participants (see details in Table 1) was invited to measure the in-plane unsaturated permeability of a carbon fabric using their respective setups and following the guidelines of this benchmark. As the unidirectional method was chosen, three directions of measurement were necessary to obtain the in-plane ellipse of permeability [14]. Thus, nine institutions were able to carry out these measurements and obtain the permeability ellipse. This paper presents the procedure used, the experimental conditions adhered to and the results obtained by each participant. These results were analyzed and compared in order to determine the scatter of values occurring when following the given guidelines. Finally, a short comparison with the first benchmark is carried out.

Table 1 – Participants in the benchmark exercise.

Institution	Division	Country	Referred to as
École Polytechnique de Montréal	Chair on Composites of High Performance	Canada	CCHP
Technische Universität Clausthal	Institut für Polymerwerkstoffe und Kunststofftechnik	Germany	Clausthal
University of Delaware	Department of Mechanical Engineering	USA	Delaware
National University of Mar del Plata	Institute of Material Science and Technology	Argentina	INTEMA
École Polytechnique Fédérale de Lausanne	Laboratoire de Technologie des Composites et Polymères	Switzerland	Lausanne
KU Leuven	Departement of Metallurgy and Materials Engineering	Belgium	Leuven
University of Wisconsin	Department of Mechanical Engineering	USA	Milwaukee
Technische Universität Munich	Institue for Carbon Composites	Germany	Munich
University of Nottingham	Division of Materials, Mechanics and Structures	United Kingdom	Nottingham
Pôle Plasturgie de l'Est	Centre technique international de mise en oeuvre de matériaux composites	France	PPE
SICOMP	Swerea	Sweden	Sicomp
Universitat Politècnica de Valencia	Instituto de Technologia de Materiales	Spain	Valencia
Eidgenössische Technische Hochschule Zürich	Centre of Structure Technologies	Switzerland	Zurich

2. Permeability measurement

2.1. Material specifications

Reinforcement

As in the first permeability benchmark, the reinforcement chosen is a 2x2-twill carbon fabric provided by Hexcel Fabrics with an areal density of 285 g/m^2. It is composed of 6K fiber tows in both warp and weft directions. These tows are equally spaced in both directions. The fabric properties are summarized in Table 2. The fabric measurements were performed according to ISO 10120:1991 and ISO 3801:1977.

Table 2 – Details on reinforcement architecture.

Manufacturer	Hexcel Fabrics	
Fabric	G0986 D1200 Carbon fabric	
	Data sheet	Measured
Weave	2x2 twill	
Areal density (g/m²)	285	284 ± 2
Fiber density (g/m³)	1.78e^6	
Nominal construction (tows/cm)	Warp : 3.5 Weft : 3.5	3.52 ± 0.07 3.46 ± 0.07
Weight distribution	Warp : 50% Weft : 50%	
Tows warp and weft	Carbon HT	
Type	HTA 5131 6K	
Filament diameter (μm)	7	
Linear density (tex)	400	419 ± 15
Tow width (mm)	n/a	Warp 2.31 ± 0.17 Weft 2.27 ± 0.20
Image		

As displayed in Figure 1, testing directions at 0° and 90° were defined respectively in the warp and weft of the roll. The 45° testing orientation was obtained between the 0° and 90° counter clockwise. This upfront definition allows the comparison of the unidirectional effective permeability of all participants.

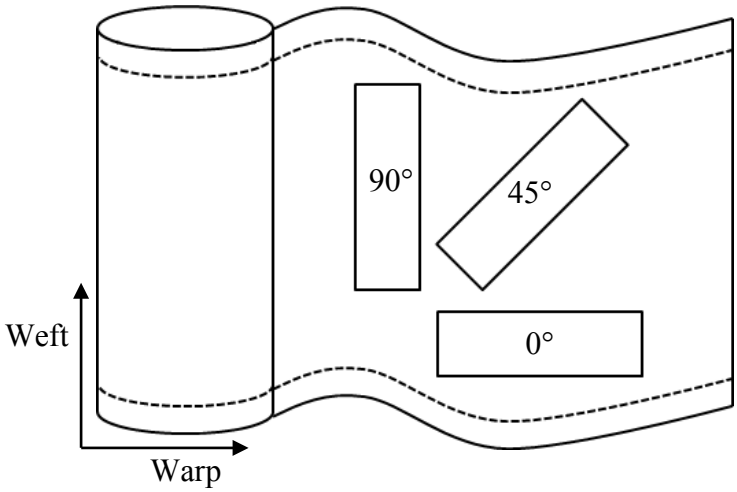

Figure 1 – Directions for cutting in the reinforcement roll.

Test fluid

Thermosetting resins typically used in composite manufacturing show a Newtonian behavior prior to gelation. However, viscosity may vary due to solvent evaporation or cure reaction. Thus, the use of a test fluid instead of resin is usually recommended in order to perform experiments in a more reproducible manner. For this reason, a silicone oil was recommended as the testing fluid for this benchmark. Table 3 summarizes the test fluids used by each participant of the exercise. Only three participants have chosen a different fluid: corn syrup for Delaware, motor oil for Milwaukee and a Petro-Canada synthetic oil for Nottingham. Fluid properties were verified by most participants before the experiments. The majority of them have also verified the Newtonian behavior of the test fluid. The targeted viscosity of the fluid was fixed to 0.1 Pa · s. The effective viscosity varied between 0.088 and 0.220 Pa · s as given in Table 3.

Table 3 – List of testing fluids used by each participant.

Institution	Test fluid	Determination of viscosity	Temperature (°C)	Viscosity (Pa.s)	Additional comments
CCHP	Silicone oil	T measured before test μ from $\mu(T)$ curve	23 to 23.9	0.100 to 0.101	Newtonian behavior verified
Clausthal	Silicone oil	μ from $\mu(T)$ curve	18.6 to 23.8	0.096 to 0.104	Newtonian behavior verified
Delaware	Corn syrup	-	23.1 to 23.3	0.098 to 0.160	-
INTEMA	Silicone oil	T measured before test μ from $\mu(T)$ curve	-	0.106 to 0.122	-
Lausanne	Silicone oil	T measured before test μ from $\mu(T)$ curve	21.5 to 22	0.088	Newtonian behavior verified
Milwaukee	Motor oil	T measured before test μ from $\mu(T)$ curve	20.5 to 23	0.200 to 0.220	-
Munich	Silicone oil	T measured before test μ from $\mu(T)$ curve	12.4 to 21	0.124 to 0.142	Newtonian behavior verified
Nottingham	Petro-Canada Synthetic oil	T measured before test μ from $\mu(T)$ curve	20 to 21.5	0.095 to 0.103	Newtonian behavior verified
PPE	Silicone oil	-	-	0.100	-
Sicomp	Silicone oil	T measured before test μ from $\mu(T)$ curve	18.5 to 19.8	0.100	Newtonian behavior verified
Valencia	Silicone oil	-	25.5	0.100	-
Zurich	Silicone oil	T measured before test μ from $\mu(T)$ curve	25 to 26.9	0.102 to 0.105	Newtonian behavior verified

2.2. Test setups

In this study, test setups were composed of two rigid mold surfaces as a standard RTM (Resin Transfer Molding) mold. Top molds were transparent (acrylic, glass, etc.) to be able to observe the fluid flowing through the reinforcement while bottom molds were opaque (aluminum or steel). Between these two parts, the thickness was fixed using frames or shims as shown schematically in Figure 2. A sealing rubber was also placed between the mold surfaces in order to prevent any leak during the measurement. The test fluid was injected from the injection gate on one side of the sample along the longitudinal direction of the mold. The setup used by each participant is detailed in Table 4.

Sample size is another key parameter that has to be chosen wisely. The size of the fibrous material must be several times larger than the unit cell of the woven fabric. In fact, sample size has to be larger than the Representative Elementary Volume (REV) of the fabric. Moreover, the ratio length versus width of the sample plays an important role since a sample that is too wide will lead to a radial flow that diverges from the unidirectional condition required. For a good uniformity, a minimal dimension of 400 mm in length and

100 mm in width was suggested for this study. A fixed fiber volume fraction (V_f) of 45% was also suggested for these tests. The number of fabric layers also influences the permeability value. Fiber nesting and non-uniform compaction of the layers cause the intra tow spaces to differ for different numbers of stacked layers. To reduce variability, the number of layers and hence the mold cavity thickness were fixed for this experiment. A total of 10 layers was suggested for each direction as well as a cavity height of 3.5 mm in order to obtain a V_f close to 45%. Some of the participants could not obtain this cavity thickness due to their existing setups. Hence, the number of layers in the preform was adjusted in order to be as close as possible to the desired fiber volume fraction (see Table 4).

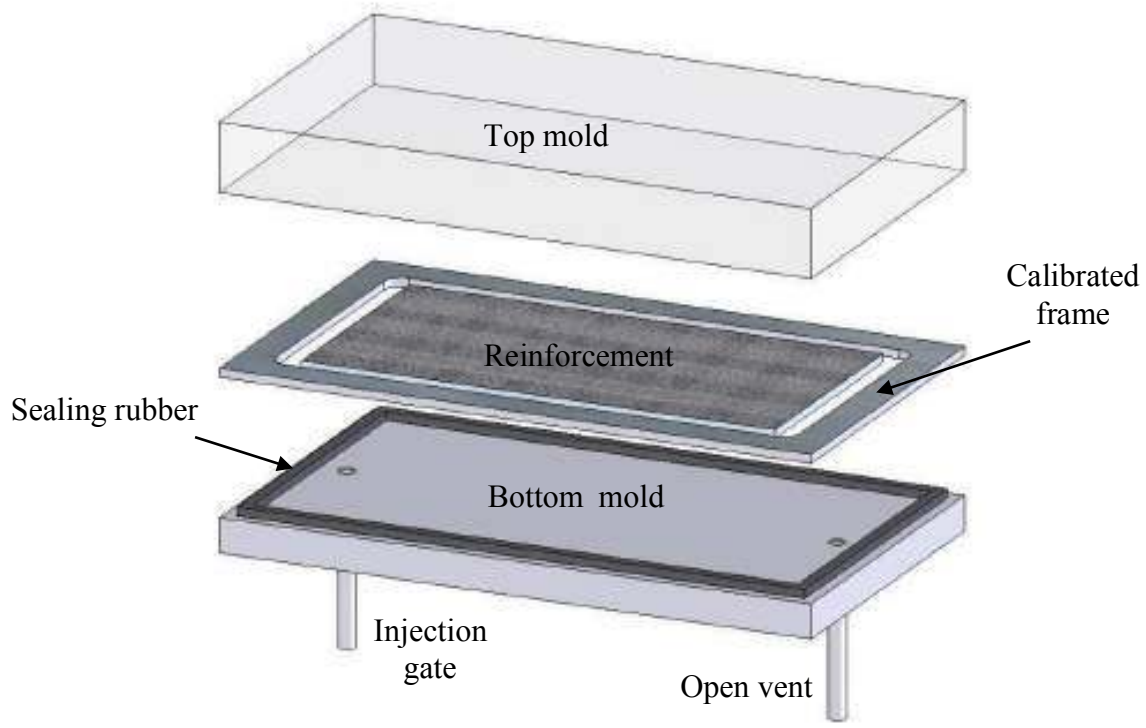

Figure 2 – Typical test mold as described in [23].

When measuring the unsaturated permeability of a dual scale porous media, one must pay special attention to the flow velocity at the flow front. Saturation of the fabric is a combination of the Stokes flow happening along the intra tow spaces and the capillary flow inside the tows. The unsaturated permeability of the fabric is then a consequence of the Stokes versus capillary flow ratio. Varying the injection pressure has a direct impact on the fluid velocity and hence on the unsaturated permeability value of the fabric. To ensure testing the fibers under same flow conditions, an average capillary number has to be chosen (see equation (3)):

$$\mathrm{Ca} = \frac{\mu \cdot v_f}{\gamma \cdot cos\theta} \quad (3)$$

where v_f is the flow velocity, θ the contact angle between the resin and the fibers and γ the surface tension of the resin. Since the test fluid has already been fixed as a silicone oil with similar properties for all participants (i.e. similar μ, γ and θ), the only parameter left is the flow velocity which depends on injection pressure. It was hence reasonable to define a common injection pressure for all participants. It was agreed that an injection pressure of 1 bar would be representative of the processing of the carbon fabric to be tested. As presented in Table 5, most participants measured an injection pressure between 0.85 and 1.85 bars. Only Milwaukee used a constant flow rate injection unit that did not allow controlling pressure.

In this exercise, there was no particular specification regarding the flow front detection. Numerous techniques exist to perform the flow front tracking such as the use of fiber optic sensors [24], pressure transducers [25] or ultrasound measurement [26]. However, the most commonly employed method remains the visual monitoring through a transparent mold [14, 27]. In order to reduce the scatter and solve statistical equations described in the next section, it was recommended to measure multiple data points during testing. As displayed in Table 5, most of the participants have opted for the visual tracking of the flow front. Nottingham has chosen a pressure transducer to detect the flow front position in a closed mold. In this case, only one data point per test was available to compute the permeability. Milwaukee has injected the testing fluid at a constant flow rate. Thus, the saturated permeability was estimated by measuring the pressure drop across the preform. Neither Milwaukee nor Nottingham was able to apply the equations presented below.

2. Permeability measurement

2.1. Material specifications

Reinforcement

As in the first permeability benchmark, the reinforcement chosen is a 2x2-twill carbon fabric provided by Hexcel Fabrics with an areal density of 285 g/m^2. It is composed of 6K fiber tows in both warp and weft directions. These tows are equally spaced in both directions. The fabric properties are summarized in Table 2. The fabric measurements were performed according to ISO 10120:1991 and ISO 3801:1977.

Table 2 – Details on reinforcement architecture.

Manufacturer	Hexcel Fabrics	
Fabric	G0986 D1200 Carbon fabric	
	Data sheet	Measured
Weave	2x2 twill	
Areal density (g/m²)	285	284 ± 2
Fiber density (g/m³)	1.78e^6	
Nominal construction (tows/cm)	Warp : 3.5 Weft : 3.5	3.52 ± 0.07 3.46 ± 0.07
Weight distribution	Warp : 50% Weft : 50%	
Tows warp and weft	Carbon HT	
Type	HTA 5131 6K	
Filament diameter (μm)	7	
Linear density (tex)	400	419 ± 15
Tow width (mm)	n/a	Warp 2.31 ± 0.17 Weft 2.27 ± 0.20
Image		

As displayed in Figure 1, testing directions at 0° and 90° were defined respectively in the warp and weft of the roll. The 45° testing orientation was obtained between the 0° and 90° counter clockwise. This upfront definition allows the comparison of the unidirectional effective permeability of all participants.

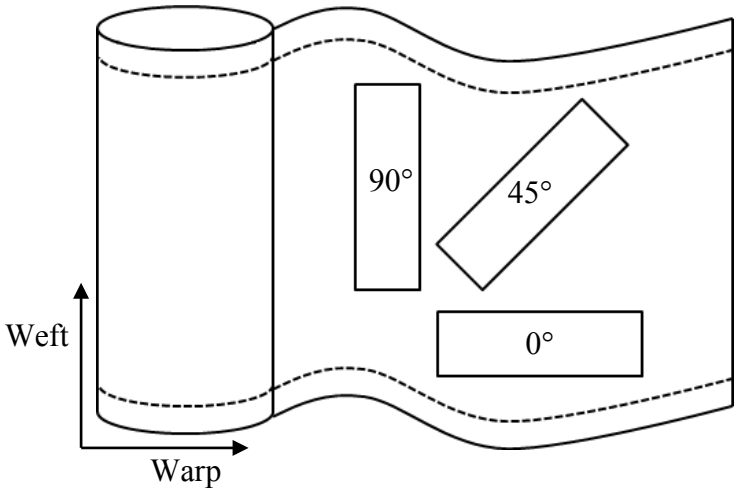

Figure 1 – Directions for cutting in the reinforcement roll.

Test fluid

Thermosetting resins typically used in composite manufacturing show a Newtonian behavior prior to gelation. However, viscosity may vary due to solvent evaporation or cure reaction. Thus, the use of a test fluid instead of resin is usually recommended in order to perform experiments in a more reproducible manner. For this reason, a silicone oil was recommended as the testing fluid for this benchmark. Table 3 summarizes the test fluids used by each participant of the exercise. Only three participants have chosen a different fluid: corn syrup for Delaware, motor oil for Milwaukee and a Petro-Canada synthetic oil for Nottingham. Fluid properties were verified by most participants before the experiments. The majority of them have also verified the Newtonian behavior of the test fluid. The targeted viscosity of the fluid was fixed to 0.1 Pa · s. The effective viscosity varied between 0.088 and 0.220 Pa · s as given in Table 3.

Table 3 – List of testing fluids used by each participant.

Institution	Test fluid	Determination of viscosity	Temperature (°C)	Viscosity (Pa.s)	Additional comments
CCHP	Silicone oil	T measured before test μ from $\mu(T)$ curve	23 to 23.9	0.100 to 0.101	Newtonian behavior verified
Clausthal	Silicone oil	μ from $\mu(T)$ curve	18.6 to 23.8	0.096 to 0.104	Newtonian behavior verified
Delaware	Corn syrup	-	23.1 to 23.3	0.098 to 0.160	-
INTEMA	Silicone oil	T measured before test μ from $\mu(T)$ curve	-	0.106 to 0.122	-
Lausanne	Silicone oil	T measured before test μ from $\mu(T)$ curve	21.5 to 22	0.088	Newtonian behavior verified
Milwaukee	Motor oil	T measured before test μ from $\mu(T)$ curve	20.5 to 23	0.200 to 0.220	-
Munich	Silicone oil	T measured before test μ from $\mu(T)$ curve	12.4 to 21	0.124 to 0.142	Newtonian behavior verified
Nottingham	Petro-Canada Synthetic oil	T measured before test μ from $\mu(T)$ curve	20 to 21.5	0.095 to 0.103	Newtonian behavior verified
PPE	Silicone oil	-	-	0.100	-
Sicomp	Silicone oil	T measured before test μ from $\mu(T)$ curve	18.5 to 19.8	0.100	Newtonian behavior verified
Valencia	Silicone oil	-	25.5	0.100	-
Zurich	Silicone oil	T measured before test μ from $\mu(T)$ curve	25 to 26.9	0.102 to 0.105	Newtonian behavior verified

2.2. Test setups

In this study, test setups were composed of two rigid mold surfaces as a standard RTM (Resin Transfer Molding) mold. Top molds were transparent (acrylic, glass, etc.) to be able to observe the fluid flowing through the reinforcement while bottom molds were opaque (aluminum or steel). Between these two parts, the thickness was fixed using frames or shims as shown schematically in Figure 2. A sealing rubber was also placed between the mold surfaces in order to prevent any leak during the measurement. The test fluid was injected from the injection gate on one side of the sample along the longitudinal direction of the mold. The setup used by each participant is detailed in Table 4.

Sample size is another key parameter that has to be chosen wisely. The size of the fibrous material must be several times larger than the unit cell of the woven fabric. In fact, sample size has to be larger than the Representative Elementary Volume (REV) of the fabric. Moreover, the ratio length versus width of the sample plays an important role since a sample that is too wide will lead to a radial flow that diverges from the unidirectional condition required. For a good uniformity, a minimal dimension of 400 mm in length and

100 mm in width was suggested for this study. A fixed fiber volume fraction (V_f) of 45% was also suggested for these tests. The number of fabric layers also influences the permeability value. Fiber nesting and non-uniform compaction of the layers cause the intra tow spaces to differ for different numbers of stacked layers. To reduce variability, the number of layers and hence the mold cavity thickness were fixed for this experiment. A total of 10 layers was suggested for each direction as well as a cavity height of 3.5 mm in order to obtain a V_f close to 45%. Some of the participants could not obtain this cavity thickness due to their existing setups. Hence, the number of layers in the preform was adjusted in order to be as close as possible to the desired fiber volume fraction (see Table 4).

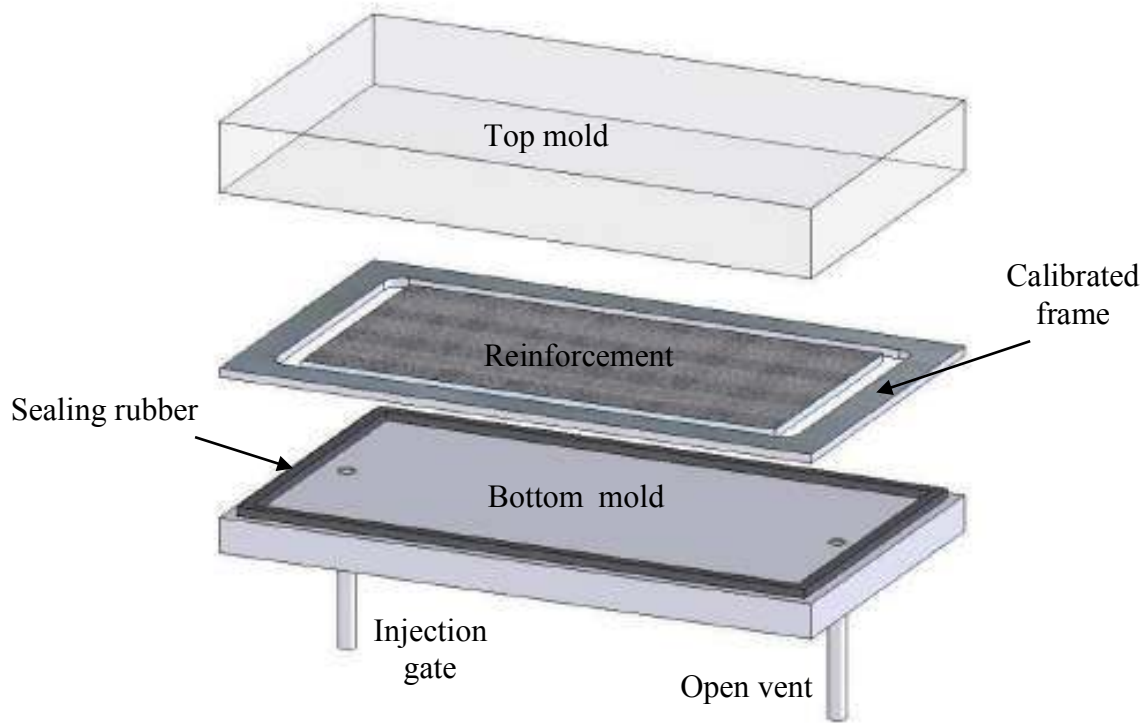

Figure 2 – Typical test mold as described in [23].

When measuring the unsaturated permeability of a dual scale porous media, one must pay special attention to the flow velocity at the flow front. Saturation of the fabric is a combination of the Stokes flow happening along the intra tow spaces and the capillary flow inside the tows. The unsaturated permeability of the fabric is then a consequence of the Stokes versus capillary flow ratio. Varying the injection pressure has a direct impact on the fluid velocity and hence on the unsaturated permeability value of the fabric. To ensure testing the fibers under same flow conditions, an average capillary number has to be chosen (see equation (3)):

$$\mathrm{Ca} = \frac{\mu \cdot v_f}{\gamma \cdot cos\theta} \quad (3)$$

where v_f is the flow velocity, θ the contact angle between the resin and the fibers and γ the surface tension of the resin. Since the test fluid has already been fixed as a silicone oil with similar properties for all participants (i.e. similar μ, γ and θ), the only parameter left is the flow velocity which depends on injection pressure. It was hence reasonable to define a common injection pressure for all participants. It was agreed that an injection pressure of 1 bar would be representative of the processing of the carbon fabric to be tested. As presented in Table 5, most participants measured an injection pressure between 0.85 and 1.85 bars. Only Milwaukee used a constant flow rate injection unit that did not allow controlling pressure.

In this exercise, there was no particular specification regarding the flow front detection. Numerous techniques exist to perform the flow front tracking such as the use of fiber optic sensors [24], pressure transducers [25] or ultrasound measurement [26]. However, the most commonly employed method remains the visual monitoring through a transparent mold [14, 27]. In order to reduce the scatter and solve statistical equations described in the next section, it was recommended to measure multiple data points during testing. As displayed in Table 5, most of the participants have opted for the visual tracking of the flow front. Nottingham has chosen a pressure transducer to detect the flow front position in a closed mold. In this case, only one data point per test was available to compute the permeability. Milwaukee has injected the testing fluid at a constant flow rate. Thus, the saturated permeability was estimated by measuring the pressure drop across the preform. Neither Milwaukee nor Nottingham was able to apply the equations presented below.

Table 4 – Details on tool setup used by participants.

Institution	Sample size (mm²)	Length/width ratio	Thickness (mm)	Number of layers	Tool material	Reported closing/deflection
CCHP	400*100	4.0	3.60	10	Steel (bottom) Glass (top)	Thickness variation: 1.1 %
Clausthal	240*120	2.0	3.50	10	Steel (bottom) Glass (top) + steel stiffeners	Thickness variation: ≤ 1 %
Delaware	457*142	3.2	3.18	10	Aluminium (bottom) Acrylic (top) + steel stiffening structure	-
INTEMA	400*100	4.0	3.50	10	Steel (bottom) Glass (top)	Thickness variation: 1.4 % Mold deflection: 0.1 %
Lausanne	250*63	4.0	2.84	8	Steel (bottom) Glass (top))+steel frame	Thickness variation: 1.8 % Mold deflection: 0.1 %
Milwaukee	1200*178	6.7	10.00	28	Aluminum (bottom) Lexan (top)	Thickness variation: 0.5 % Mold deflection: ≤ 0.1 %
Munich	380*192	2.0	3.50	10	Steel, 35 mm (bottom) Polycarbonate, 40 mm (top)	
Nottingham	280*114.5	2.5	3.50	10	Steel, 25.3 mm (bottom) Perspex, 25.6 mm (top)	Thickness variation: 0.9%
PPE	300*100	3	3.50	10	Aluminum (bottom) Polycarbonate (top)	Thickness variation: ≤ 2% Mold deflection: ≤ 2 %
Sicomp	300*150	2.0	3.50	10	Steel, 25 mm (bottom) Acrylic, 80 mm (top)	Thickness variation: 0.4 % Mold deflection: max 1 %
					Aluminum, 20 mm (bottom)	

structure

Table 5 – Details on injection pressures and flow detection techniques.

Institution	Monitoring injection pressure	Initial injection pressure (bar)	Final injection pressure (bar)	Flow detection	Sensitivity
CCHP	Measured at injection gate	0.85 to 1.08	0.88 to 1.11	Human eye + photos	0.5 sec.
Clausthal	-	0.86	0.86	Photos + Software	Photos every 5 sec
Delaware	Measured at pressure pot	1.00	1.00	Video	-
INTEMA	Measured at pressure pot	0.84 to 1.38	0.85 to 1.58	Human eye	0.5 sec.
Lausanne	Measured at injection gate	0.60 to 1.20	0.60 to 1.29	Human eye	0.5 sec.
Milwaukee	Flow rate measured at injection gate	Q=4.4 ml/sec.	-	-	-
Munich	Measured at injection gate	0.91 to 1.12	1.07 to 1.40	Human eye	0.5 sec.
Nottingham	Measured at injection gate	1.02 to 1.13	1.02 to 1.13	Pressure transducer	0.5 sec.
PPE	Measured at injection gate	1.01	1.02	Video	0.5 sec.
Sicomp	Measured at injection gate	0.97 to 1.00	0.88 to 0.97	Human eye + video	0.5 sec.
Valencia	Measured at injection gate	0.86 to 1.16	1.01 to 1.28	Human eye + photos	0.5 sec.
Zurich	Measured at injection gate	0.93 to 0.97	0.93 to 0.97	Human eye + photos	Photos every 2 sec.

2.3. Permeability calculations

To calculate the permeability of a fibrous reinforcement, it is important to know and control the fiber volume fraction of the preform. This fiber volume fraction is directly connected to the total mass of fiber m_f (of all the fabric layers), the length l and the width w of the preform, the mold cavity height h and the volumetric density of the fiber ρ_f:

$$V_f = \frac{m_f}{l \cdot w \cdot h \cdot \rho_f} \tag{4}$$

The free porosity Φ of the fibrous reinforcement can be thus calculated as:

$$\Phi = 1 - V_f \tag{5}$$

Unidirectional permeability calculation

Two different techniques were used to determine the unidirectional permeability of the fabric in each direction. Both methods require injecting the test fluid at a constant pressure P_{inj}. The first one is based on an interpolation of the flow front position during the injection. According to Darcy's law, a linear trend can be fitted when plotting the squared flow front position against the time. The permeability of a fibrous reinforcement can then be computed as follows:

$$K_{\mathrm{SFF}} = \frac{x_{ff}^2 \cdot \Phi \cdot \mu}{2P_{\mathrm{inj}} \cdot t} = \frac{\mathrm{m} \cdot \Phi \cdot \mu}{2\ P_{\mathrm{inj}}} \tag{6}$$

where x_{ff} corresponds to the flow front position at the instant t, which can be replaced by the slope m interpolated from the coupled data $\left(x_{ff}^2, t\right)$. This approach will be referred to in this paper as the Squared Flow Front method (SFF method).

The second technique used to compute the unidirectional permeability is based on a statistical approximation of the experimental data. As described by Ferland et al. [28], a least square fit can be applied to the values of pressure in order to estimate a permeability self-correlated to Darcy's law. Indeed, defining:

$$a = \sqrt{\frac{2\ K}{\Phi\ \mu}} \tag{7}$$

and applying a least square fit on the approximated integral of the pressure gives:

$$a = \frac{\sum_{i=1}^{n} x_{ff,i}\sqrt{I_i}}{\sum_{i=1}^{n} I_i} \tag{8}$$

with:

$$I_i = I_{i-1} + \frac{\left(P_{\text{inj},i} - P_{\text{inj},i-1}\right)}{2}\left(t_i - t_{i-1}\right) \tag{9}$$

Finally, the Least Square Fit permeability (LSF method) is determined substituting equation (8) in (7):

$$K_{\text{LSF}} = \frac{\left(\frac{\sum_{i=1}^{n} x_{ff,i}\sqrt{I_i}}{\sum_{i=1}^{n} I_i}\right)^2 \cdot \Phi \cdot \mu}{2} \tag{10}$$

Principal permeability calculation

Once the unidirectional permeability of the fibrous reinforcement in the three different directions (0°, 45° and 90°) is obtained, it is possible to calculate the in-plane permeability tensor K_1 and K_2 as follows [14]:

$$K_1 = K_{\text{exp}}^{0}\frac{\alpha_1 - \alpha_2}{\alpha_1 - \frac{\alpha_2}{\cos(2\beta)}} \tag{11}$$

and

$$K_2 = K_{\text{exp}}^{90}\frac{\alpha_1 + \alpha_2}{\alpha_1 + \frac{\alpha_2}{\cos(2\beta)}} \tag{12}$$

where α_1 and α_2 are written as:

$$\alpha_1 = \frac{K_{\text{exp}}^{0} + K_{\text{exp}}^{90}}{2} \tag{13}$$

$$\alpha_2 = \frac{K_{\text{exp}}^{0} - K_{\text{exp}}^{90}}{2} \tag{14}$$

and the orientation β of the ellipse is:

$$\beta = \frac{1}{2}\tan^{-1}\left(\frac{\alpha_1}{\alpha_2} - \frac{{\alpha_1}^2 - {\alpha_2}^2}{\alpha_2 \cdot K_{\exp}^{45}}\right) \quad (15)$$

Error calculation

The uncertainty on K_1, K_2 and β can be estimated according to two different methods: using the law of error propagation [25] or using the exact total differential. Both methods have advantages and drawbacks: the former is easy to calculate but depends on values not always easy to estimate while the latter depends only on effective experimental values of permeability but is more complex to develop. In the first benchmark, the law of error propagation was applied. However, uncertainties on several principal permeability data were not calculated because some information was missing. In this work, for a better comparison, the exact total differentials were calculated for K_1, K_2 and β. Equation (16) displays the exact total differential of β.

$$d\beta = \left|\frac{\partial\beta}{\partial K_{\exp}^{0}}\right| \cdot dK_{exp}^{0} + \left|\frac{\partial\beta}{\partial K_{\exp}^{45}}\right| \cdot dK_{\exp}^{45} + \left|\frac{\partial\beta}{\partial K_{\exp}^{90}}\right| \cdot dK_{\exp}^{90} \quad (16)$$

with, for example:

$$\frac{\partial\beta}{\partial K_{\exp}^{0}} = \frac{K_{\exp}^{45} \cdot K_{\exp}^{90}\left(K_{\exp}^{90} - K_{\exp}^{45}\right)}{\left[{K_{\exp}^{45}}^2\left({K_{\exp}^{0}}^2 + {K_{\exp}^{90}}^2\right) + 2K_{\exp}^{0} \cdot K_{\exp}^{90}\left(K_{\exp}^{0} \cdot K_{\exp}^{90} - K_{\exp}^{45}\left(K_{\exp}^{0} + K_{\exp}^{90}\right)\right)\right]} \quad (17)$$

The results obtained were compared with the law of propagation for the values obtained by Nottingham. Uncertainties obtained were comparable in both cases even if the law of propagation was slightly more conservative.

3. Results and discussion

3.1. Reinforcement deformability

The permeability measurements were completed by the characterization of the deformability of the fabric carried out by the KU Leuven. This information may in future be helpful to improve the interpretation of the permeability data or to carry out numerical simulations. Shear testing was done using a picture frame [29, 30], compression testing was done on the undeformed and sheared fabrics. The results are shown in Figure 3. The important deformability features of the studied fabric are:

- very low shear resistance, which up to a shear angle of 45° is completely defined by low friction in the yarn intersections

- locking shear angle above 50°
- pronounced nesting effect, with a decrease of the effective thickness of the ply in a four-plies laminate by15-20% compared to one-ply thickness

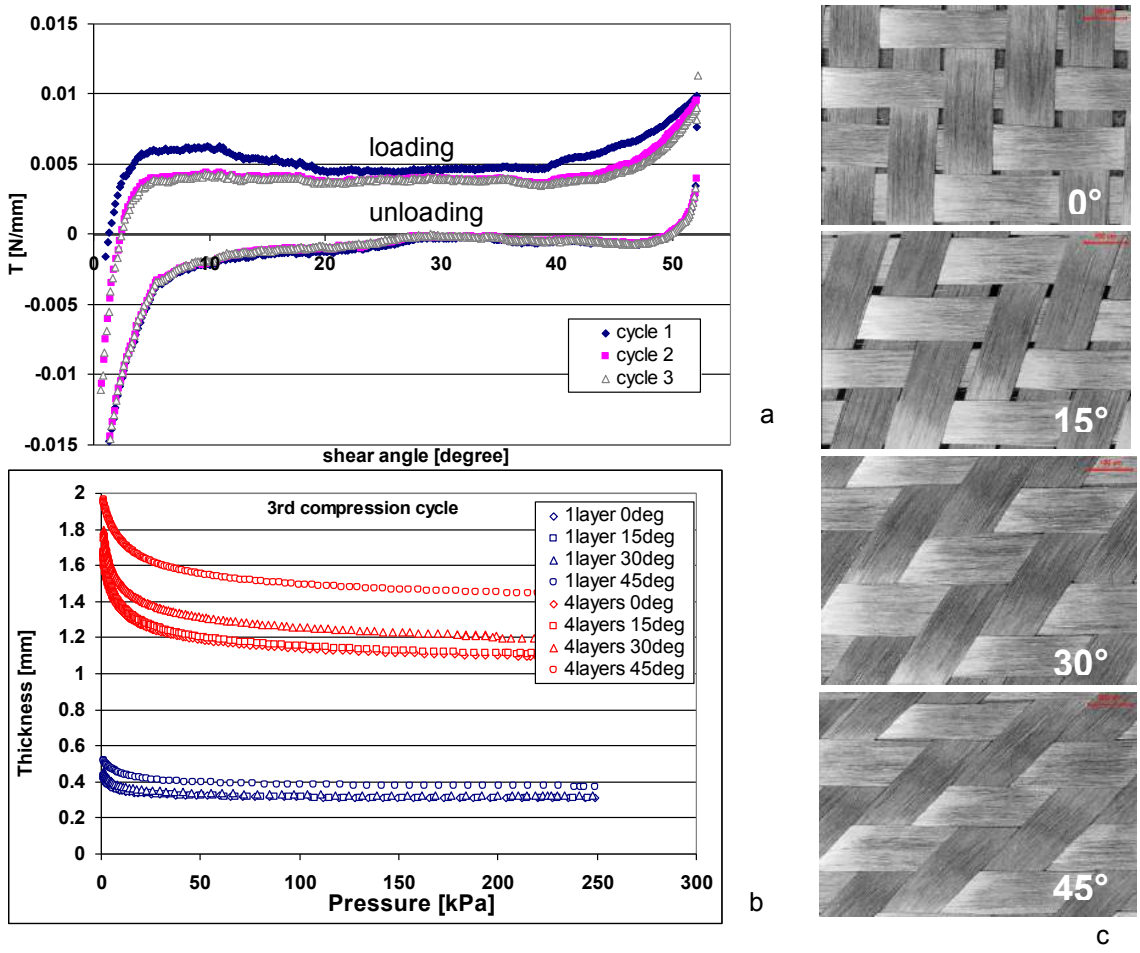

Figure 3 Fabric deformability: (a) shear diagrams: shear force *T* vs shear angle; (b) compression diagrams: fabric thickness vs. pressure (c) images of the sheared fabric;

3.2. Effective permeability results

The effective permeabilities measured by all participants are displayed in Figures 5 to 7 and data presented in Tables 6 to 8. All the participants have used the SFF and LSF methods to calculate the permeability in each direction except for Nottingham and Milwaukee. They have used their own formula as their setup is different from that of other institutions (see section 2.2 for details). For Nottingham, only one calculation of permeability was available (based on the single point method in [28]) while for Milwaukee, two values were obtained: in the steady-state condition (in SFF column) and in the transient condition (in LSF column). The choice to put these values in these columns is arbitrary but does not affect the comparison since they are almost identical.

Tables 6 to 8 also present two different arithmetic means calculated as follows: a) the average permeability values of participants who respected the recommendations (all institutions except Delaware, Nottingham and Milwaukee) and b) the average permeability values of all participants (except Milwaukee). Data obtained by Milwaukee are approximately one order of magnitude higher than that of the other participants. Thus, these results were not used in the mean value of all participants. Regarding Figures 5 to 7, the unique value obtained by Nottingham is displayed in both the SFF and LSF graphs. As for the calculated mean in the tables, the values for Milwaukee are not shown in these figures because of the significant deviation from the rest of the results. For two participants (Lausanne and Milwaukee), the average value and standard deviation were calculated despite only two experiments having been performed in each direction. This statistical evaluation of the data is questionable since permeability measurements have a significant variability. A greater number of tests were carried out from other institutions allowing better statistical evaluation.

Results at 0°

Figures 4 (a) and (b) show respectively to the results obtained at 0° with the SFF and LSF methods as presented in Table 6. For both methods, the permeability values of participants respecting the recommendations are very close, with a lower variability for the LSF method. For these eight institutions, the scatter may represent the uncertainty of the fiber volume fraction, fiber nesting and the testing technique. When respecting the guidelines, the estimated error on the standard deviation is only ±22% for the SFF method and ±19% for LSF, which is very low considering that these tests were carried out by nine different institutions. Coefficients of variation calculated for each participant from their own data is generally around 15%. It means that the variability observed between each setup is almost comparable to the variability of the setups themselves in this direction.

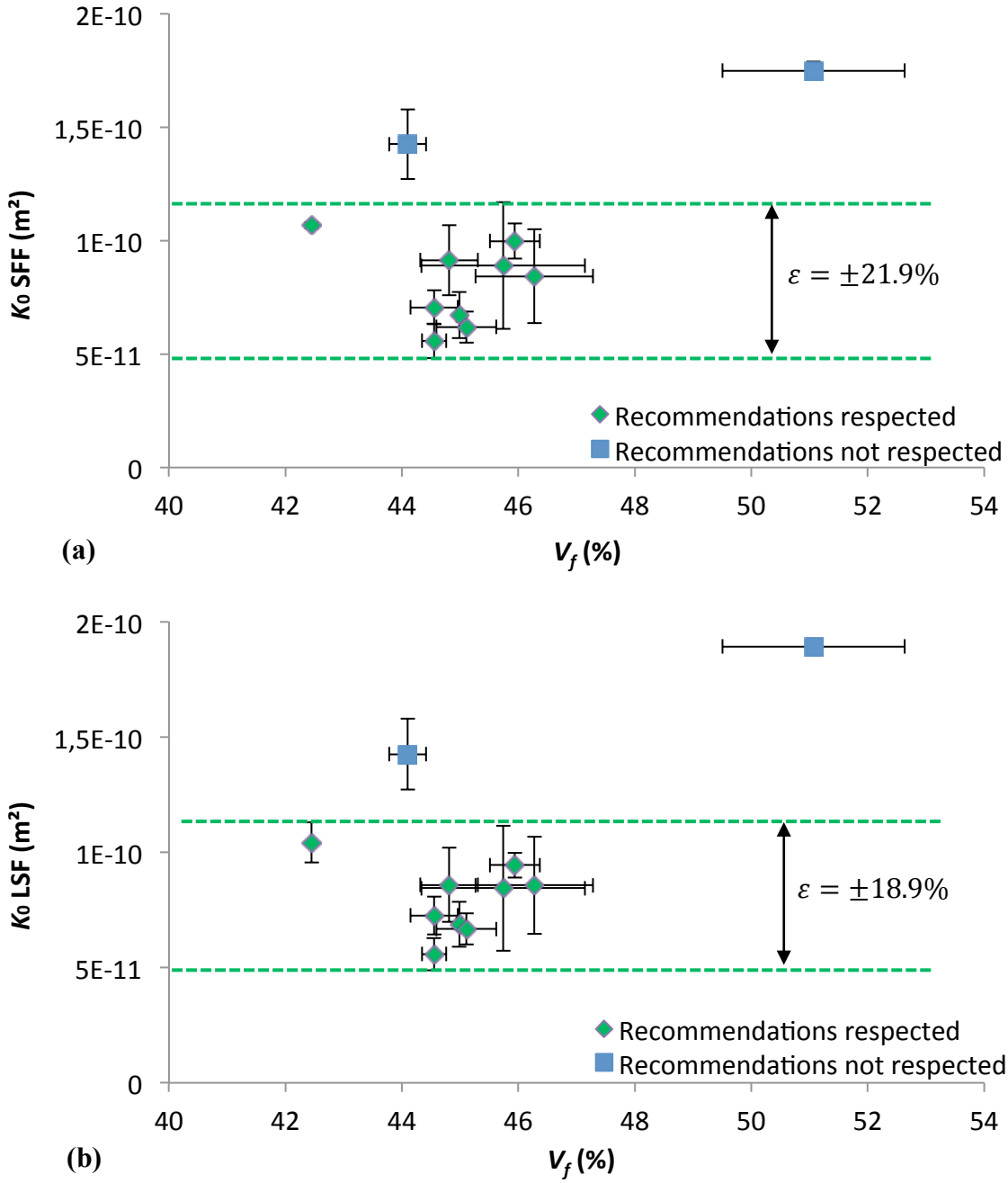

Figure 4 – Effective permeability at 0° calculated using: (a) the SFF method and (b) the LSF method.

Results at 45°

Displayed in Figures 5 (a) and (b) are the results obtained at 45° with the SFF and LSF methods respectively. These results are also available in Table 7. Even if less data are available in this direction, some interesting remarks can be inferred: again, SFF and LSF methods give comparable results with less scatter for the LSF method. The standard deviations of the permeability in this direction are lower than at 0°. Some participants had difficulties to control the fiber volume fraction of the samples, probably because the cutting

of the fabric posed problem. Indeed, as presented in the previous section on reinforcement characterization, the fabric can be sheared very easily until an angle of almost 40°. Cutting the sample at 45° is then more laborious than at 0° or 90° since the fabric shears during cutting, thus varying the areal density of the sample and consequently the fiber volume fraction. The scatter of experimental data in this direction is in the same range as for the effective permeability at 0°. The coefficient of variation in this direction is comparable to the one obtained at 0° (around 22%). The value obtained by Nottingham is still slightly higher than that of other participants' results.

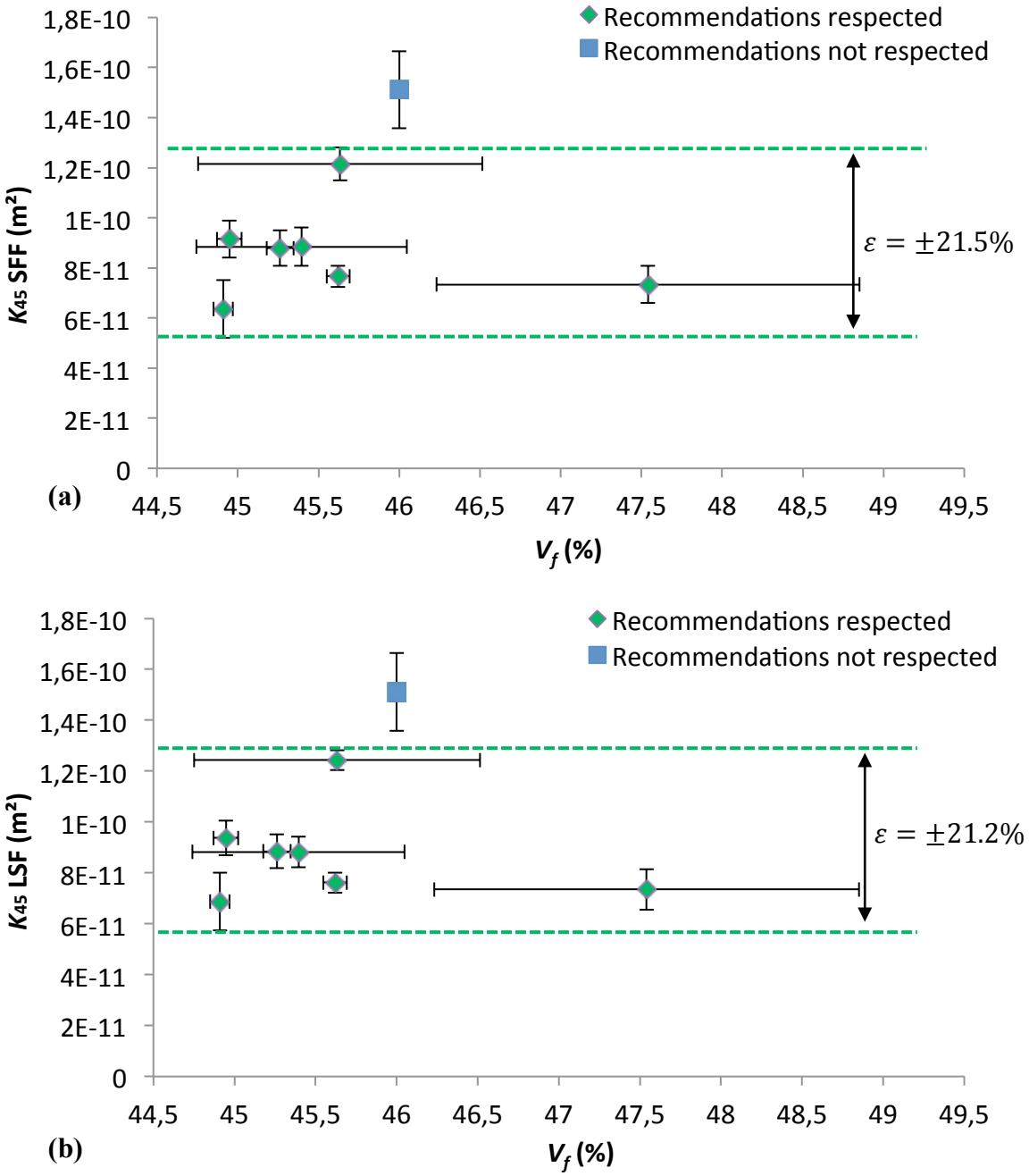

Figure 5 – Effective permeability at 45° calculated using: (a) the SFF method and (b) the LSF method.

Results at 90°

Figures 6 (a) and (b) show the permeability results at 90° obtained with the SFF and LSF methods respectively. These values are also available in Table 8. Both methods give comparable results with again lower scatter for the LSF method. In this direction, a higher variation of fiber volume fraction is observed. In fact, five values are near 45% while other results are around 42% and 48%. However, the variability between institutions is about the same as at 0° and 45° (coefficient of variation on the mean around 21%). The permeability values obtained by Nottingham and Delaware are slightly higher than those from the other participants. However these institutions did not respect the recommendations due to their existing setup.

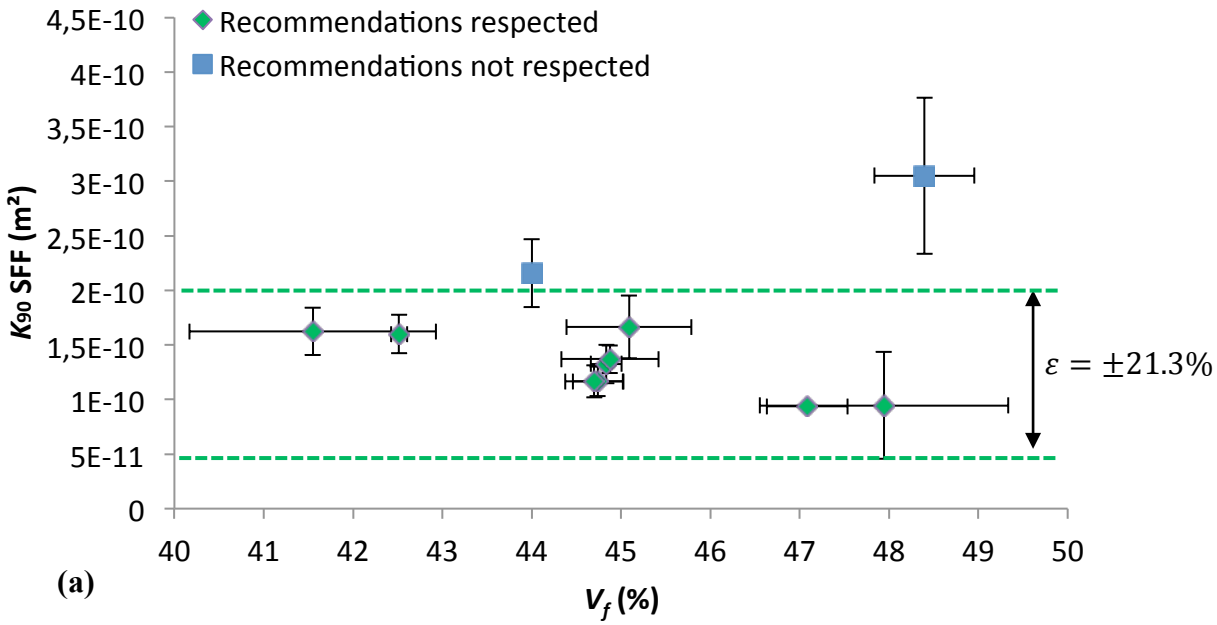

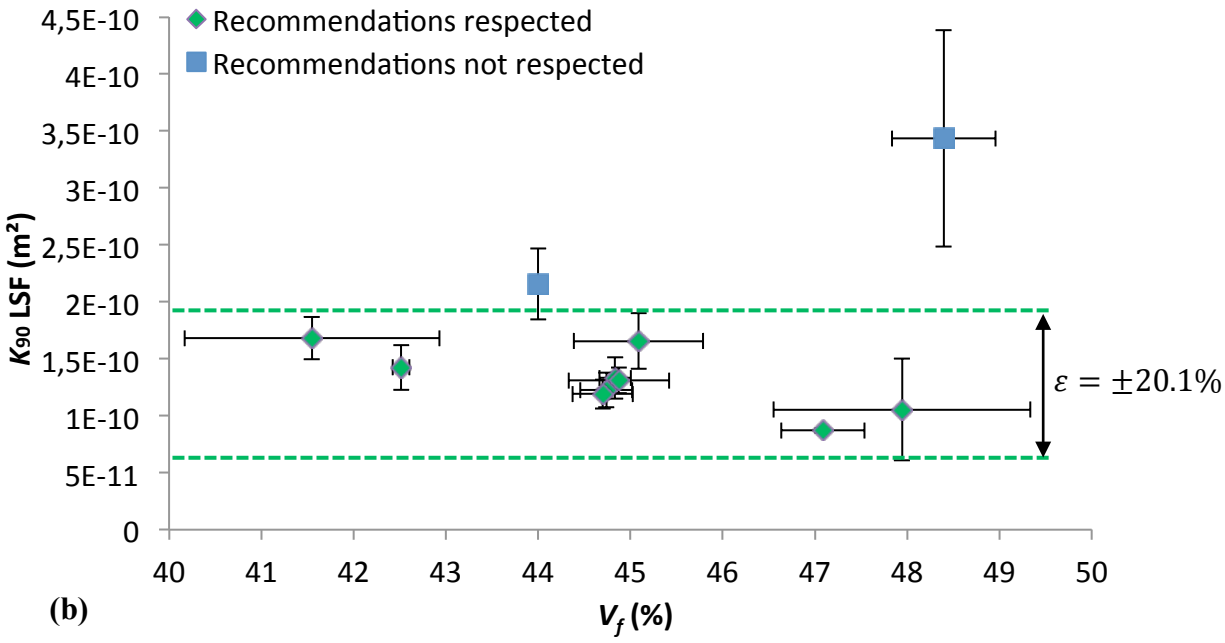

Figure 6 – Effective permeability at 90° calculated using: (a) the SFF method and (b) the LSF method.

General remarks

As mentioned previously, the SFF and LSF methods seem to give similar results for each direction. The LSF technique systematically shows a lower dispersion than the SFF method. The coefficient of variation observed for the mean values of permeability of each participant when the recommendations are respected is around 15% for each direction. The coefficient of variation considering all institutions is also very low (around 21%). The scatter between each institution is comparable to the scatter of each institution, which suggests robustness of the proposed technique to characterize the permeability of fibrous reinforcements.

As already observed in the first benchmark, results obtained from setups with different specifications contrast those from setups that respect the guidelines of the present benchmark. Milwaukee obtained permeabilities one order of magnitude higher while Delaware and Nottingham obtained values around 1.5 to 2.7 times higher. This difference may arise from the way the permeability is calculated for Milwaukee and Nottingham, but not for Delaware. The constant flow rate procedure used by Milwaukee is hardly comparable to others. The method of flow front detection is different for Nottingham and the permeability calculation is based on the single point method. The only common difference with other participants is the injected fluid. In fact, all the other institutions have used silicone oil while Delaware, Milwaukee and Nottingham have used corn syrup, motor

oil and Petro-Canada synthetic oil respectively. Despite this observation, it cannot be concluded here that the testing fluid is responsible for the scatter observed. New measurements on the same setup using silicone oil may validate this hypothesis.

3.3. Principal permeability results

To calculate the in-plane permeability tensor of the fabric, it is necessary to have unidirectional permeability measurements in each of the three directions (i.e. 0°, 45° and 90°). Thus, participants who have not performed tests in all the three directions could not obtain the permeability tensor. Hence, only eight institutions were able to provide sufficient data to perform tensor calculations.

In Figures 7 to 10, values of K_1, K_2, K_1/K_2 and β for each participant are displayed respectively. The error bars displayed in these figures are calculated using equation (16). Tables 9 and 10 summarize these data for the SFF and LSF approaches respectively. At the bottom of these tables the average values of participants who respected the recommendations (all institutions except Delaware, Nottingham and Milwaukee) and the average values of all participants (except Milwaukee) are presented.

Principal permeability K_1

Figures 7 (a) and (b) show the principal permeability K_1 calculated from effective permeabilities obtained via the SFF and LSF methods respectively. The exact values are available in Tables 9 and 10. An averaged permeability K_1 of $1.4\text{x}10^{-10}$ m² was obtained for all participants that respected the guidelines of this exercise. This result is similar for both approaches used to compute effective permeabilities, SFF and LSF. However, the LSF approach gives lower scatter than the SFF approach (22% for SFF versus 20% for LSF).

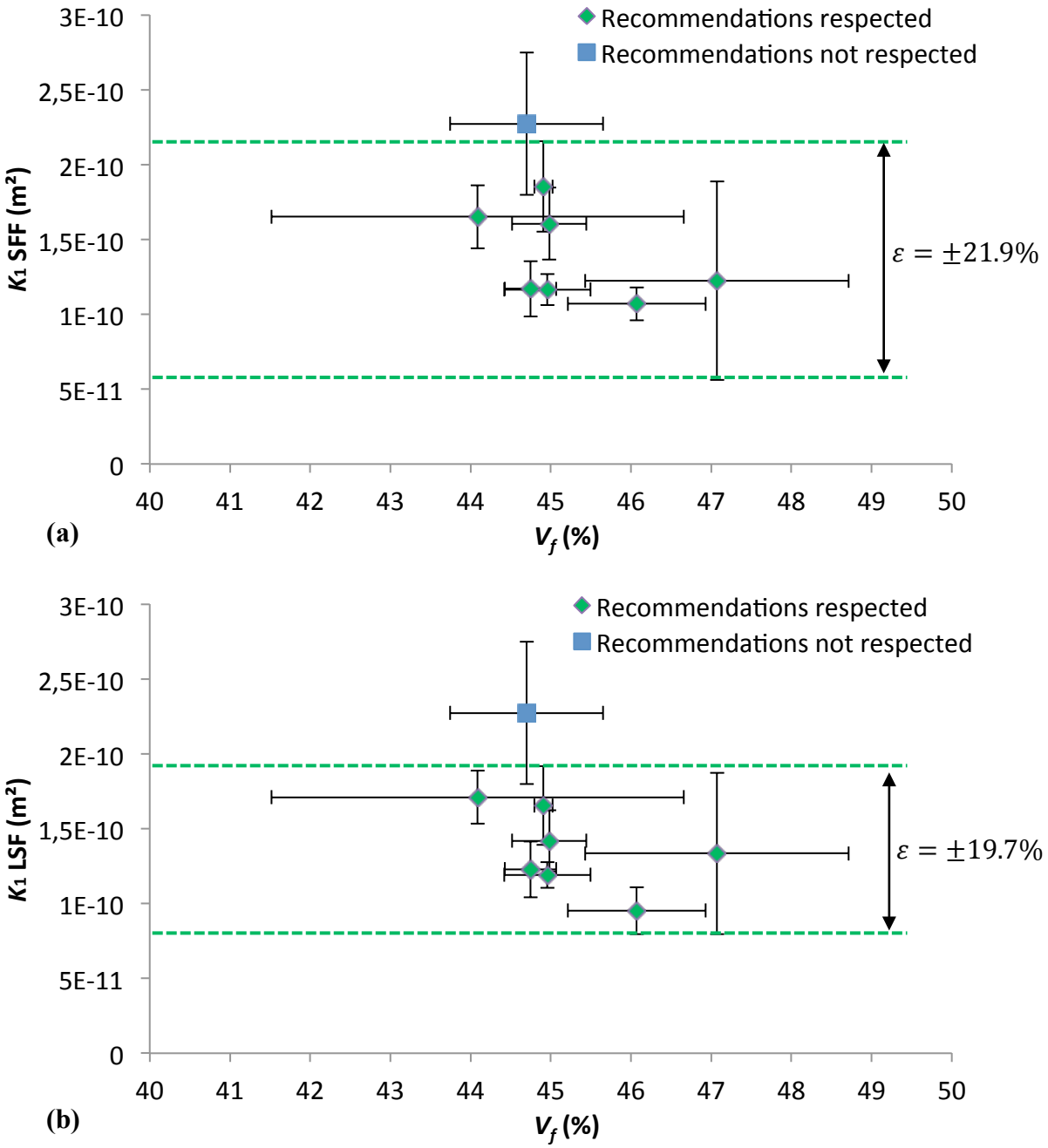

Figure 7 – Principal permeability K_1 obtained using: (a) the SFF method and (b) the LSF method.

Principal permeability K_2

The principal permeability K_2 calculated from effective permeabilities obtained via the SFF and LSF methods for each participant is displayed in Figures 8 (a) and (b) respectively. The exact values are also available in Tables 9 and 10. An averaged principal permeability K_2 of $7.3\text{x}10^{-11}$ m² was obtained from both SFF and LSF approaches. Permeability K_2 is half the value of K_1. This will be analyzed in the K_1/K_2 anisotropy ratio section. These results show that the LSF method still yields less scatter of experimental data.

The coefficient of variation of data obtained respecting the recommendations is low (around 16%). It confirms that the scatter of the values for these seven institutions is negligible in relation to the scatter of values of the experiments conducted at each department.

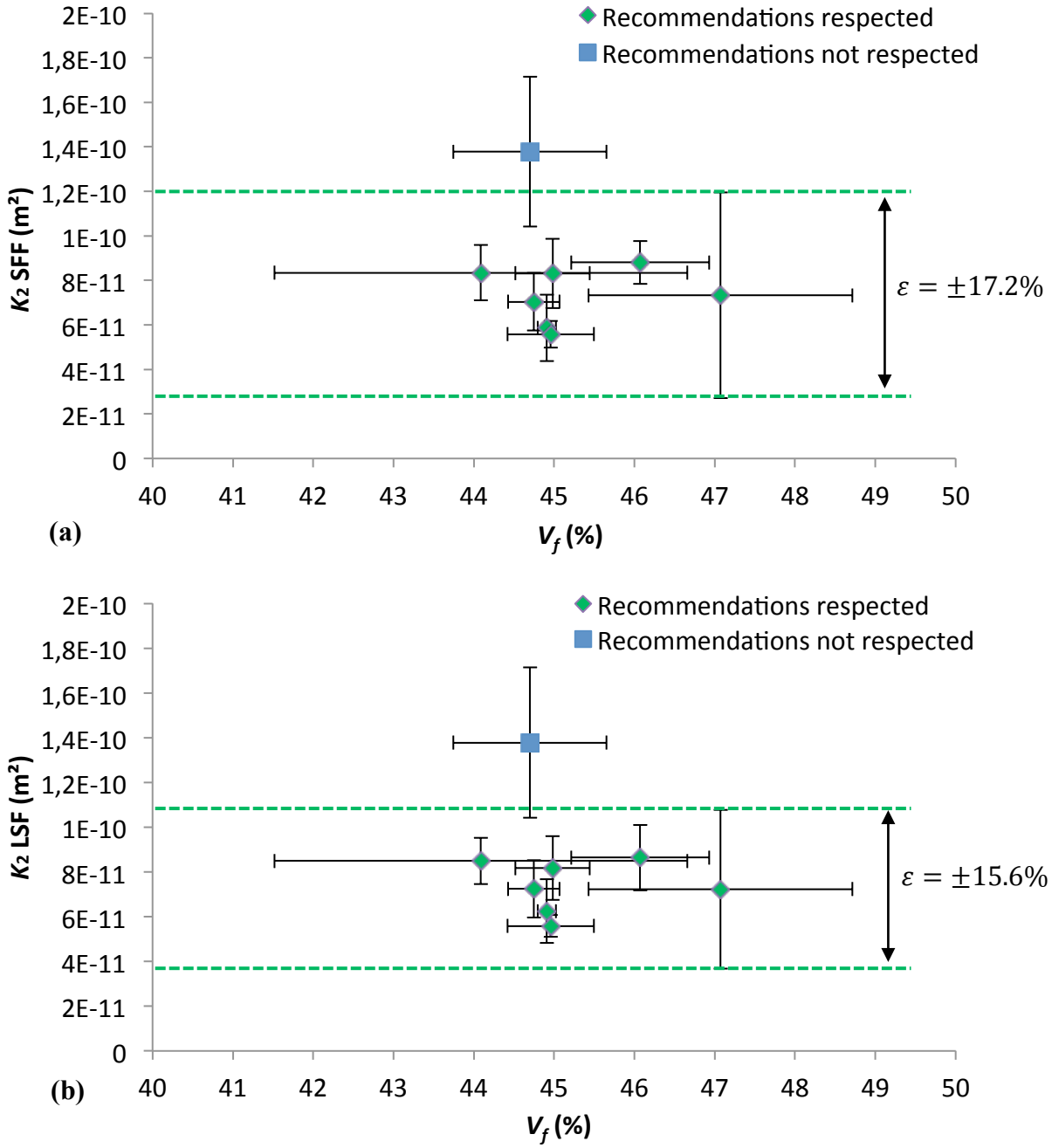

Figure 8 – Principal permeability K_2 obtained using: (a) the SFF method and (b) the LSF method.

Anisotropy ratio K_1/K_2

Ratios of anisotropy calculated from the values of principal permeabilities are shown in Figure 9 (a) for the SFF approach and Figure 9 (b) for the LSF method. Values are

available in Tables 9 and 10 respectively. The scatter between institutions for the LSF calculation is much lower than using SFF (31% for SFF and 25% for LSF).

The LSF approach has shown to produce less scatter over the effective permeabilities than the SFF approach and hence it also results in a better determination of the permeability tensor and the elliptic shape of the in-plane flow.

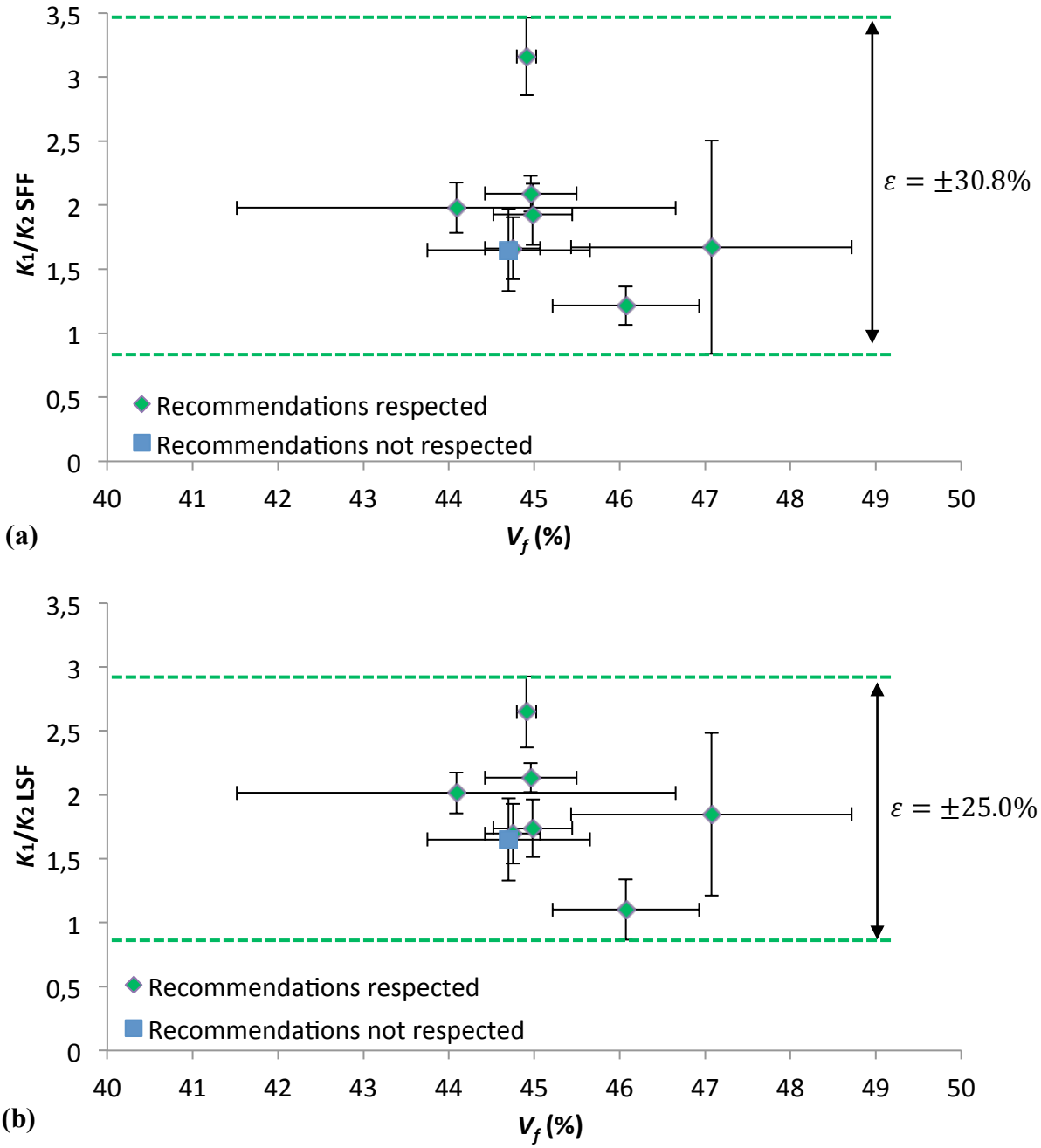

Figure 9 – Anisotropy ratio K_1/K_2 obtained using: (a) the SFF method and (b) the LSF method.

Ellipse orientation β

The orientation angle β between the warp direction and the major axis of permeability K_1 for each participant is shown in Figures 10 (a) and (b) for the SFF and LSF approaches respectively. Experimental data are also available in Tables 9 and 10. The averaged elliptic flow determined by each institution is around 96°. The variability of the flow orientation from most participants is in the order of ±20°. However, this is not the case for Sicomp, for which a variability of ±37° was observed. This is probably related to the lack of control of V_f and shearing deformation of the fabric during cutting as explained in section 3.2. Despite this higher variability, the averaged flow directions are still close to other participants' results. As for previous results, the LSF approach results in smaller variability than the SFF technique, although both give the same orientation.

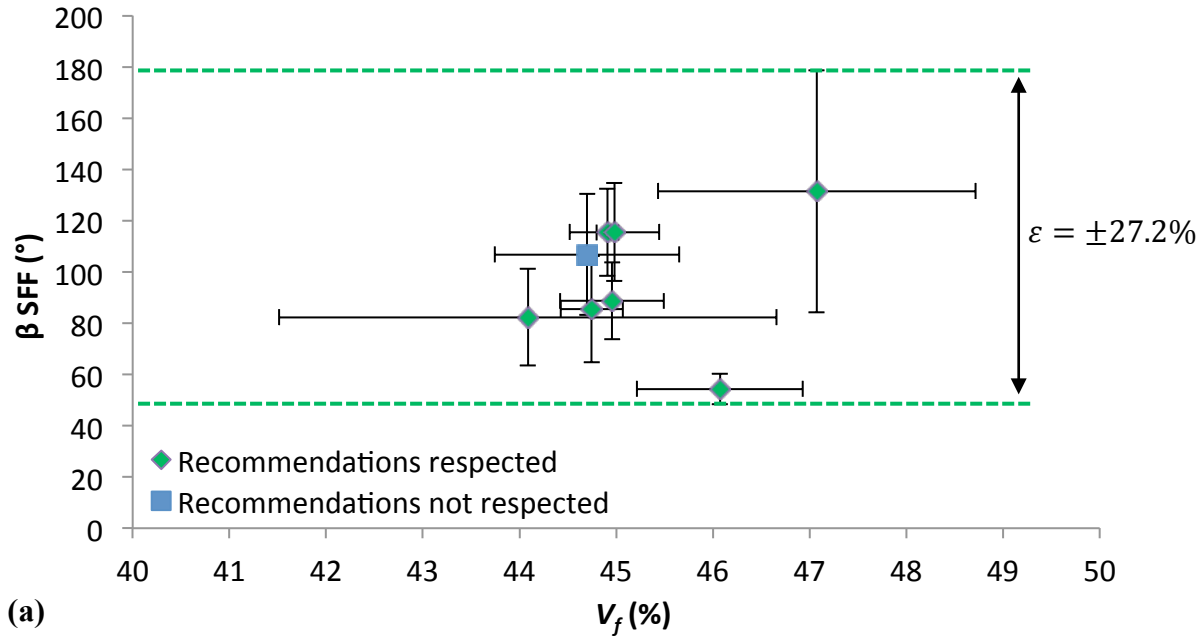

(a)

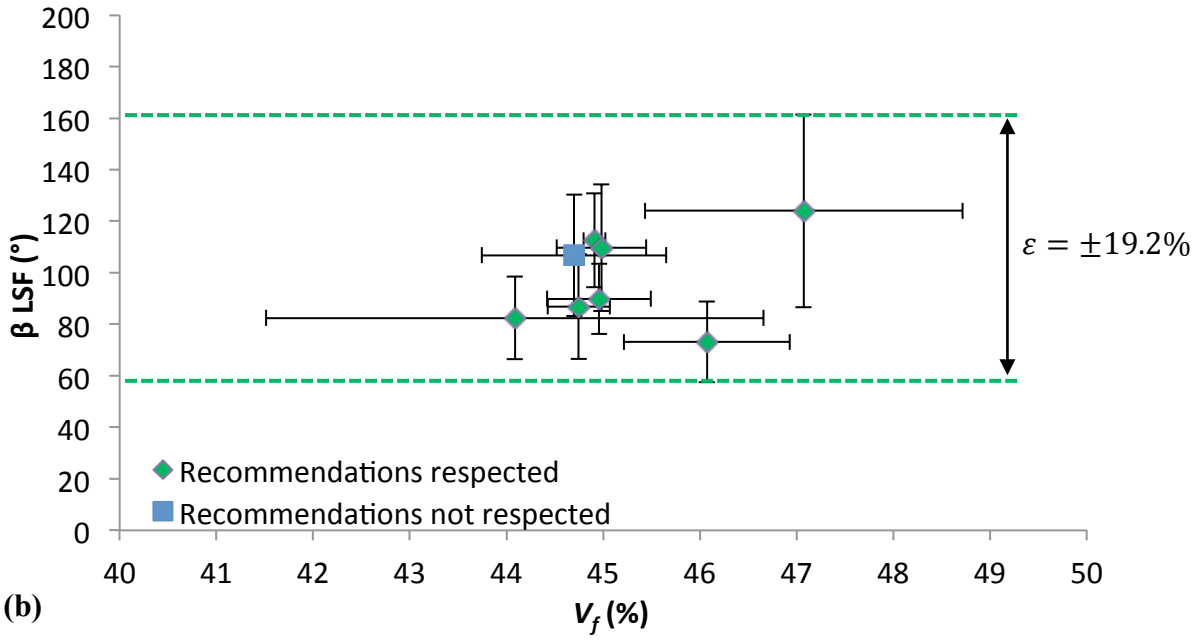

Figure 10 – Angle β obtained using: (a) the SFF method and (b) the LSF method.

4. Comparison with the first permeability benchmark

In the first permeability benchmark exercise [21], a total of 16 different characterization techniques were compared, such as radial or linear injection, saturated or unsaturated flow, constant pressure or flow rate, with different test fluids. Each participant was asked to measure permeability using his current set-up and practice. Figures 11 and 12 display the results of K_1 and K_2 obtained for the first benchmark. The compilation of results from twelve institutions resulted in a high variability of data: permeabilities measured at similar V_f varied by more than one order of magnitude. In the conclusions of that benchmark, authors suspected that human factor could be responsible for this significant scatter.

The present exercise, based on a common characterization technique used by eight different institutions, shows a very small scatter compared to the first benchmark. The variability observed in the second benchmark is also displayed on Figures 11 and 12 for comparison. It can be first stated that the average permeability obtained in the second exercise is nearly one order of magnitude smaller than for the first benchmark at a fiber volume fraction of 45%. The scatter of experimental data is also 1 order of magnitude smaller in the second exercise. This applies to the principal permeabilites K_1 and K_2. The ellipse orientation β was defined in the second benchmark as the angle between the warp direction of the fabric and the major axis of permeability. In the first benchmark, it was described as the angle between the weft direction of the fabric and the major axis. Thus, to compare both results,

90° has to be added to the angle calculated in the first benchmark. Finally, an ellipse orientation of approximately 90° was found in both benchmarks.

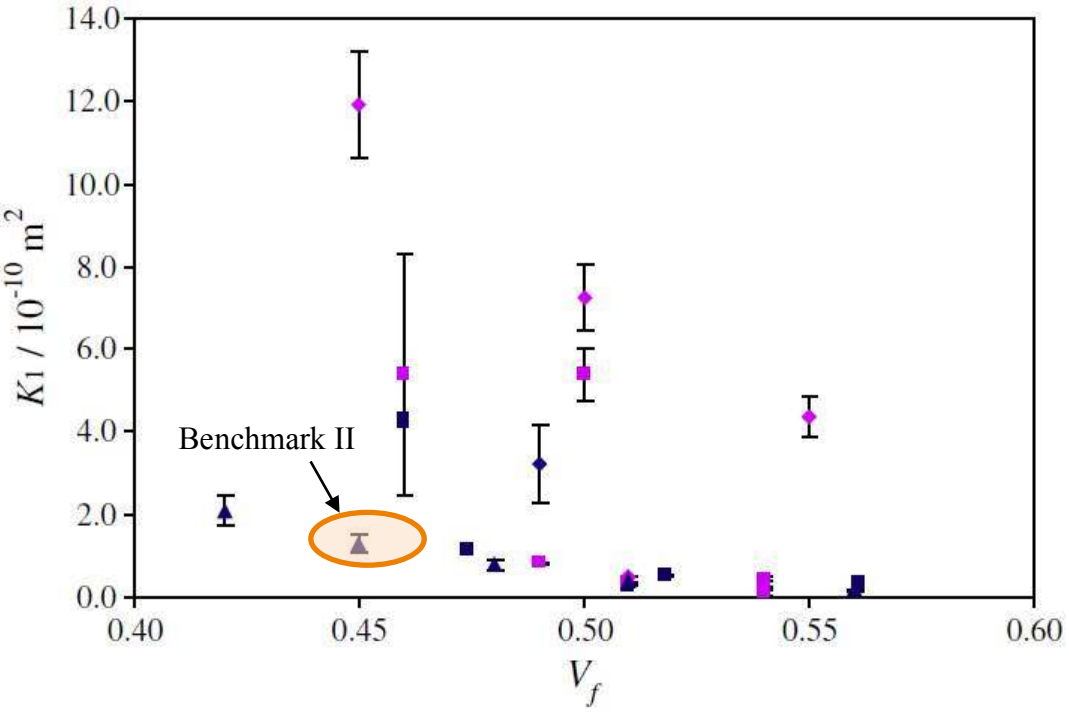

Figure 11 – Principal permeability K_1 obtained in the first permeability benchmark [21].

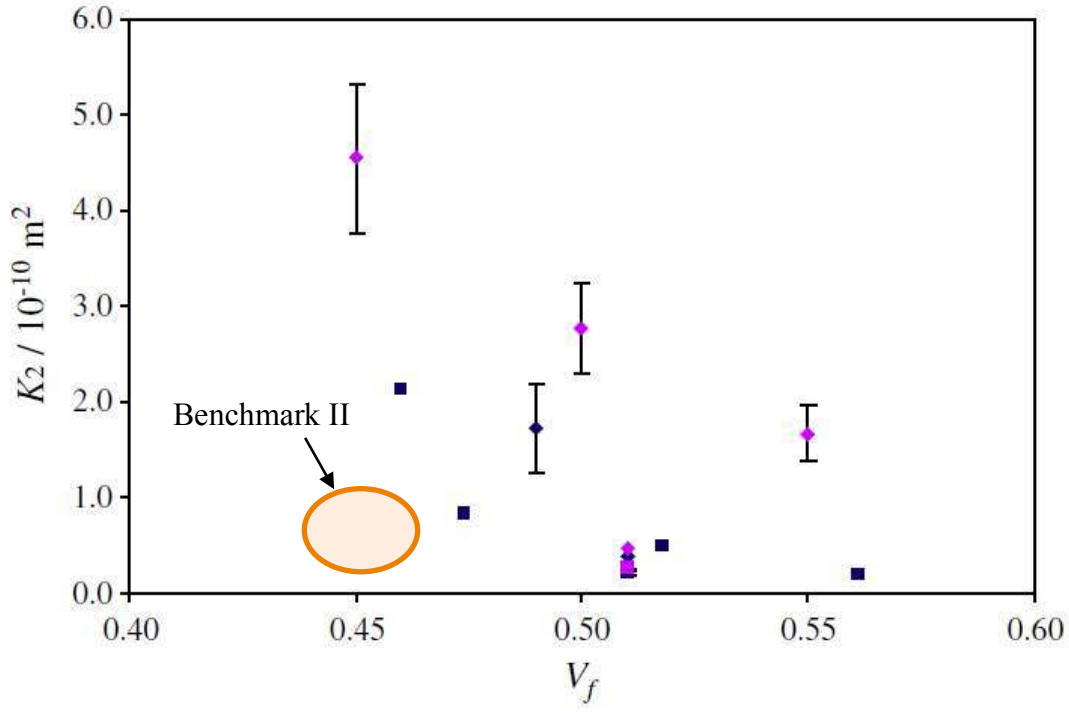

Figure 12 – Principal permeability K_2 obtained in the first permeability benchmark [21].

5. Conclusion

The aim of this second permeability benchmark was to measure and compare the permeability of a carbon fabric using a specified procedure. A total of 13 institutions have participated on this exercise worldwide. One institution has investigated the geometrical parameters and deformations of the chosen carbon fabric while others have measured and reported the in-plane permeability.

The unidirectional unsaturated permeability of the fabric has been characterized in three specific directions (0°, 45° and 90°). Parameters such as test fluid, injection pressure, fiber volume fraction, etc. were fixed in order to ensure high reproducibility. Defining the test fluid is mainly based on the fact that capillary flow plays a key role on the saturation of fiber tows and hence on the unsaturated permeability values. This was done by specifying the test fluid as silicone oil with a viscosity of 0.1 Pa·s, and the injection pressure of 1 bar. In addition, sample dimensions, aspect ratio and fiber volume fraction were also specified for the proposed exercise.

A series of templates was created so that each participant carried out the permeability calculations according to the same set of formulas. Finally, experimental data from participating institutions were compiled and presented in this paper.

As a result of this exercise, an averaged permeability of $1.4\text{x}10^{-10}$ m² was obtained in the principal direction of the carbon fabric. In the minor axis direction, an averaged permeability of $0.7\text{x}10^{-10}$ m² was obtained. In both cases, a scatter of ±20% was calculated from data of seven participants. Two techniques were also compared to calculate the unidirectional permeability from experimental data. The first approach called Squared Flow Front (SFF) consists of a linear regression over the square of the flow front position versus time. The second approach named Least Square Fit (LSF) uses a statistical solution to compute the permeability over a range of data. The results of this exercise demonstrate that a smaller scatter is systematically obtained when applying the LSF approach. However, in all cases, the SFF approach gave nearly the same averaged values as the LSF approach, but with a higher scatter.

From the twelve participants that reported permeability data, two of them were unable to follow the guidelines and recommendations due to limitations on their actual setups. These two institutions obtained permeability data that were significantly off the average of all

other participants. This indicates that the recommendations in the guideline document do in fact help obtain a reproducible permeability value.

Finally, a comparison was made with the first permeability benchmark carried out in 2009. This first exercise did not specify any recommendations and allowed the participants use their own specifications and setups. As a result, a large scatter of nearly 2 orders of magnitude was observed. Comparing the results of the two benchmarks, it was demonstrated that this second exercise leads to a much smaller scatter in the determination of the permeability tensor. This observation supports the assumption of this exercise that controlling the capillary number and test conditions allows reproducible characterization of the unsaturated permeability of fabrics used for composite manufacturing.

The results detailed in this article have demonstrated that a standardization of the permeability measurement is feasible. Moreover, the guidelines developed for this exercise summarize the key factors to be taken into account for proper permeability characterization. Finally, the two mathematical approaches tested in this study can both be used to compute permeability from experimental data. However, the LSF approach seems more appropriate since it systematically reduces the scatter between experiments.

6. Acknowledgements

The authors are grateful to J.M. Beraud from Hexcel Fabrics for his support that made possible this exercise. Acknowledgements are also extended to N. Vernet who was in charge of the data compilation from all the participants and had written the paper draft and presentations. The contribution of J.B. Alms, N.C. Correia, S. Advani, E. Ruiz and P.C.T. Gonçalves to the preparation of the guidelines document and templates is acknowledged by the participants of this benchmark. Contributions from T. Delavière and S. Verheyden for measurements are also acknowledged. The contribution of E. Ruiz for the organization and the supervision of this second permeability benchmark is also gratefully acknowledged.

7. Appendix

Table 6 – Effective permeabilities of each participant in direction 0°.

Institution	N_{exp}	V_f (%)	$K_{SFF0°}$ $(10^{-10}\ m^2)$	$K_{LSF0°}$ $(10^{-10}\ m^2)$
CCHP	10	44.6 ± 0.4	0.705 ± 0.074 ($\pm 10.5\%$)	0.725 ± 0.082 ($\pm 11.3\%$)
Clausthal	7	45.0 ± 0.1	0.671 ± 0.101 ($\pm 15.1\%$)	0.688 ± 0.098 ($\pm 14.3\%$)
Delaware*	3	51.1 ± 1.6	1.748 ± 0.041 ($\pm 2.4\%$)	1.892 ± 0.031 ($\pm 1.7\%$)
INTEMA	6	46.3 ± 1.0	0.842 ± 0.207 ($\pm 24.6\%$)	0.856 ± 0.210 ($\pm 24.5\%$)
Lausanne	2	42.5	1.068 ± 0.013 ($\pm 1.3\%$)	1.043 ± 0.088 ($\pm 8.4\%$)
Milwaukee*	2	45.0	8.637 ± 0.892 ($\pm 10.3\%$)	8.240 ± 0.415 ($\pm 5.0\%$)
Munich	7	44.8 ± 0.5	0.913 ± 0.154 ($\pm 16.9\%$)	0.858 ± 0.160 ($\pm 18.7\%$)
Nottingham*	10	44.1 ± 0.3	1.425 ± 0.154 ($\pm 10.8\%$)	
PPE	10	45.9 ± 0.4	0.997 ± 0.077 ($\pm 7.8\%$)	0.944 ± 0.054 ($\pm 5.7\%$)
Sicomp	10	45.7 ± 1.4	0.889 ± 0.564 ($\pm 31.4\%$)	0.844 ± 0.272 ($\pm 32.2\%$)
Valencia	10	45.1 ± 0.5	0.614 ± 0.047 ($\pm 7.6\%$)	0.683 ± 0.048 ($\pm 7.0\%$)
Zurich	9	44.6 ± 0.2	0.558 ± 0.076 ($\pm 13.7\%$)	0.558 ± 0.070 ($\pm 12.6\%$)
Mean (reco. resp.)		44.9 ± 1.1	0.807 ± 0.177 ($\pm 21.9\%$)	0.798 ± 0.151 ($\pm 18.9\%$)
Mean (all results)		45.4 ± 2.1	0.949 ± 0.360 ($\pm 38.0\%$)	0.955 ± 0.388 ($\pm 40.6\%$)

*Guidelines not respected

Table 7 – Effective permeabilities of each participant in direction 45°.

Institution	N_{exp}	V_f (%)	$K_{SFF45°}$ $(10^{-10}\ m^2)$	$K_{LSF45°}$ $(10^{-10}\ m^2)$
CCHP	10	45.0 ± 0.1	0.915 ± 0.074 ($\pm 8.0\%$)	0.937 ± 0.068 ($\pm 7.3\%$)
Clausthal	8	44.9 ± 0.1	0.635 ± 0.116 ($\pm 18.2\%$)	0.687 ± 0.113 ($\pm 16.5\%$)
Delaware*	0			
INTEMA	3	45.6 ± 0.9	1.215 ± 0.066 ($\pm 5.4\%$)	1.243 ± 0.039 ($\pm 3.2\%$)
Lausanne	0			
Milwaukee*	2	45.0	10.01 ± 0.03 ($\pm 0.2\%$)	10.01 ± 0.11 ($\pm 1.1\%$)
Munich	6	45.3 ± 0.1	0.879 ± 0.071 ($\pm 8.1\%$)	0.885 ± 0.067 ($\pm 7.6\%$)
Nottingham*	10	46.0	1.511 ± 0.153 ($\pm 10.1\%$)	
PPE	10	45.4 ± 0.7	0.885 ± 0.077 ($\pm 8.7\%$)	0.882 ± 0.060 ($\pm 6.8\%$)
Sicomp	10	47.5 ± 1.3	0.734 ± 0.164 ($\pm 10.0\%$)	0.735 ± 0.080 ($\pm 10.8\%$)
Valencia	0			
Zurich	10	45.6 ± 0.1	0.767 ± 0.043 ($\pm 5.6\%$)	0.762 ± 0.040 ($\pm 5.2\%$)
Mean (reco. resp.)		45.6 ± 0.9	0.861 ± 0.185 ($\pm 21.5\%$)	0.876 ± 0.186 ($\pm 21.2\%$)
Mean (all results)		45.7 ± 0.8	0.943 ± 0.286 ($\pm 30.4\%$)	0.955 ± 0.283 ($\pm 29.6\%$)

*Guidelines not respected

Table 8 – Effective permeabilities of each participant in direction 90°.

Institution	N_{exp}	V_f (%)	$K_{SFF90°}$ $(10^{-10}\ m^2)$	$K_{LSF90°}$ $(10^{-10}\ m^2)$
CCHP	10	44.7 ± 0.3	1.165 ± 0.135 ($\pm 11.6\%$)	1.225 ± 0.151 ($\pm 12.3\%$)
Clausthal	6	44.8 ± 0.2	1.326 ± 0.177 ($\pm 13.3\%$)	1.332 ± 0.182 ($\pm 13.6\%$)
Delaware*	5	48.4 ± 0.6	3.050 ± 0.716 ($\pm 23.5\%$)	3.435 ± 0.952 ($\pm 27.7\%$)
INTEMA	7	41.6 ± 1.4	1.623 ± 0.216 ($\pm 13.3\%$)	1.681 ± 0.186 ($\pm 11.1\%$)
Lausanne	2	42.5 ± 0.1	1.599 ± 0.177 ($\pm 11.1\%$)	1.424 ± 0.196 ($\pm 13.8\%$)
Milwaukee*	2	45.0	10.12 ± 1.31 ($\pm 13.0\%$)	11.32 ± 1.66 ($\pm 14.7\%$)
Munich	7	44.9 ± 0.6	1.369 ± 0.127 ($\pm 9.3\%$)	1.309 ± 0.112 ($\pm 8.6\%$)
Nottingham*	10	44.0	2.156 ± 0.310 ($\pm 14.4\%$)	
PPE	6	47.1 ± 0.3	0.935 ± 0.010 ($\pm 1.1\%$)	0.866 ± 0.018 ($\pm 2.1\%$)
Sicomp	10	47.9 ± 1.4	0.946 ± 1.220 ($\pm 51.7\%$)	1.055 ± 0.446 ($\pm 42.3\%$)
Valencia	10	45.1 ± 0.7	1.624 ± 0.274 ($\pm 16.9\%$)	1.644 ± 0.229 ($\pm 14.0\%$)
Zurich	8	44.7 ± 0.3	1.165 ± 0.148 ($\pm 12.7\%$)	1.191 ± 0.128 ($\pm 10.8\%$)
Mean (reco. resp.)		44.8 ± 2.0	1.311 ± 0.280 ($\pm 21.3\%$)	1.305 ± 0.262 ($\pm 20.1\%$)
Mean (all results)		45.1 ± 2.1	1.546 ± 0.613 ($\pm 39.7\%$)	1.576 ± 0.707 ($\pm 44.9\%$)

*Guidelines not respected

Table 9 – Principal permeabilities, anisotropy ratio and ellipse orientation calculated with SFF method.

Institution	V_f (%)	$K_{1\,SFF}$ ($10^{-10}\ m^2$)	$K_{2\,SFF}$ ($10^{-10}\ m^2$)	$K_{1\,SFF}/K_{2\,SFF}$	β_{SFF} (°)
CCHP	44.8 ± 0.3	1.170 ± 0.186 ($\pm 15.9\%$)	0.704 ± 0.129 ($\pm 18.3\%$)	1.663 ± 0.242 ($\pm 14.6\%$)	85.5 ± 20.8 ($\pm 24.3\%$)
Clausthal	44.9 ± 0.1	1.853 ± 0.302 ($\pm 16.3\%$)	0.587 ± 0.149 ($\pm 25.4\%$)	3.160 ± 0.301 ($\pm 9.5\%$)	115.4 ± 17.0 ($\pm 14.8\%$)
Delaware*					
INTEMA	44.1 ± 2.6	1.652 ± 0.211 ($\pm 12.8\%$)	0.835 ± 0.125 ($\pm 15.0\%$)	1.979 ± 0.197 ($\pm 10.0\%$)	82.3 ± 18.9 ($\pm 22.9\%$)
Lausanne					
Milwaukee*	45.0	10.05 ± 3.54 ($\pm 33.9\%$)	8.41 ± 3.03 ($\pm 36.0\%$)	1.242 ± 0.50 ($\pm 39.8\%$)	68.6 ± 23.6 ($\pm 34.5\%$)
Munich	45.0 ± 0.5	1.605 ± 0.241 ($\pm 15.0\%$)	0.832 ± 0.156 ($\pm 18.8\%$)	1.929 ± 0.240 ($\pm 12.4\%$)	115.5 ± 19.1 ($\pm 16.5\%$)
Nottingham*	44.7 ± 1.0	2.273 ± 0.475 ($\pm 20.9\%$)	1.378 ± 0.336 ($\pm 24.4\%$)	1.649 ± 0.321 ($\pm 19.5\%$)	106.8 ± 23.6 ($\pm 22.1\%$)
PPE	46.1 ± 0.9	1.070 ± 0.110 ($\pm 10.3\%$)	0.880 ± 0.096 ($\pm 10.9\%$)	1.215 ± 0.150 ($\pm 12.3\%$)	54.3 ± 5.9 ($\pm 10.9\%$)
Sicomp	47.1 ± 1.5	1.224 ± 0.662 ($\pm 54.1\%$)	0.733 ± 0.463 ($\pm 63.1\%$)	1.670 ± 0.831 ($\pm 49.8\%$)	131.5 ± 47.3 ($\pm 35.9\%$)
Valencia					
Zurich	45.0 ± 0.1	1.166 ± 0.104 ($\pm 8.9\%$)	0.558 ± 0.060 ($\pm 10.7\%$)	2.090 ± 0.139 ($\pm 6.7\%$)	88.7 ± 15.1 ($\pm 17.0\%$)
Mean (reco. resp.)	45.3 ± 1.0	1.391 ± 0.305 ($\pm 21.9\%$)	0.733 ± 0.126 ($\pm 17.2\%$)	1.958 ± 0.603 ($\pm 30.8\%$)	96.7 ± 26.2 ($\pm 27.2\%$)
Mean (all results)	45.2 ± 0.9	1.502 ± 0.421 ($\pm 28.0\%$)	0.813 ± 0.256 ($\pm 31.5\%$)	1.919 ± 0.569 ($\pm 29.7\%$)	97.5 ± 24.5 ($\pm 25.1\%$)

*Guidelines not respected

Table 10 – Principal permeabilities, anisotropy ratio and ellipse orientation calculated with LSF method.

Institution	V_f (%)	$K_{1\,\mathrm{LSF}}$ $(10^{-10}\ m^2)$	$K_{2\,\mathrm{LSF}}$ $(10^{-10}\ m^2)$	$K_{1\,\mathrm{LSF}}/K_{2\,\mathrm{LSF}}$	β_{LSF} (°)
CCHP	44.8 ± 0.3	1.228 ± 0.187 ($\pm 15.2\%$)	0.724 ± 0.128 ($\pm 17.7\%$)	1.696 ± 0.233 ($\pm 13.8\%$)	86.9 ± 20.3 ($\pm 23.4\%$)
Clausthal	44.9 ± 0.1	1.655 ± 0.264 ($\pm 16.0\%$)	0.625 ± 0.143 ($\pm 22.8\%$)	2.649 ± 0.279 ($\pm 10.5\%$)	112.6 ± 18.2 ($\pm 16.2\%$)
Delaware*					
INTEMA	44.1 ± 2.6	1.710 ± 0.178 ($\pm 10.4\%$)	0.849 ± 0.103 ($\pm 12.1\%$)	2.015 ± 0.160 ($\pm 7.9\%$)	82.5 ± 16.0 ($\pm 19.4\%$)
Lausanne					
Milwaukee*	45.0	11.44 ± 2.61 ($\pm 22.9\%$)	8.18 ± 2.06 ($\pm 25.2\%$)	1.400 ± 0.34 ($\pm 24.3\%$)	80.6 ± 18.3 ($\pm 22.7\%$)
Munich	45.0 ± 0.5	1.419 ± 0.205 ($\pm 14.4\%$)	0.817 ± 0.142 ($\pm 17.4\%$)	1.738 ± 0.226 ($\pm 13.0\%$)	109.8 ± 24.6 ($\pm 22.4\%$)
Nottingham*	44.7 ± 1.0	2.273 ± 0.475 ($\pm 20.9\%$)	1.378 ± 0.336 ($\pm 24.4\%$)	1.649 ± 0.321 ($\pm 19.5\%$)	106.8 ± 23.6 ($\pm 22.1\%$)
PPE	46.1 ± 0.9	0.952 ± 0.157 ($\pm 16.5\%$)	0.864 ± 0.146 ($\pm 16.9\%$)	1.102 ± 0.236 ($\pm 21.4\%$)	73.2 ± 16.7 ($\pm 21.4\%$)
Sicomp	47.1 ± 1.5	1.334 ± 0.540 ($\pm 40.5\%$)	0.723 ± 0.355 ($\pm 49.1\%$)	1.846 ± 0.636 ($\pm 34.5\%$)	124.0 ± 37.4 ($\pm 30.2\%$)
Valencia					
Zurich	45.0 ± 0.1	1.191 ± 0.087 ($\pm 7.3\%$)	0.558 ± 0.049 ($\pm 8.8\%$)	2.134 ± 0.114 ($\pm 5.4\%$)	89.8 ± 13.6 ($\pm 15.1\%$)
Mean (reco. resp.)	45.3 ± 1.0	1.356 ± 0.267 ($\pm 19.7\%$)	0.737 ± 0.115 ($\pm 15.6\%$)	1.883 ± 0.471 ($\pm 25.0\%$)	97.0 ± 18.6 ($\pm 19.2\%$)
Mean (all results)	45.2 ± 0.9	1.470 ± 0.407 ($\pm 27.7\%$)	0.817 ± 0.251 ($\pm 30.7\%$)	1.854 ± 0.444 ($\pm 24.0\%$)	98.2 ± 17.5 ($\pm 17.9\%$)

*Guidelines not respected

8. References

[1] ESI Group International Ltd, (1st november 2012). Available: http://www.esi-group.com

[2] Simacek, P. and Advani, S. G., "Modeling and simulation of resin flow in resin infusion processes such as VARTM, VAP and compression RTM", in *38th SAMPE Fall Technical Conference: Global Advances in Materials and Process Engineering, November 6, 2006 - November 9, 2006*, Dallas, TX, United states, 2006.

[3] Polyworx inc., (1st november 2012). Available: http://www.polyworx.com

[4] Darcy, H., The public fountains of the city of Dijon. Paris: Dalmont, 1856.

[5] Carman, P. C., "Fluid flow through granular beds", Transactions of the Institution of Chemical Engineers, vol. 15, pp. 150-156, 1937.

[6] Gebart, B. R., "Permeability of unidirectional reinforcements for RTM", Journal of Composite Materials, vol. 26, pp. 1100-1133, 1992.

[7] Lundström, T. S., "Permeability of non-crimp stitched fabrics", Composites Part A: Applied Science and Manufacturing, vol. 31, pp. 1345-1353, 2000.

[8] Papathanasiou, T. D., "Flow across structured fiber bundles: a dimensionless correlation", International Journal of Multiphase Flow, vol. 27, pp. 1451-61, 2001.

[9] Belov, E. B., Lomov, S. V., Verpoest, I., Peters, T., Roose, D., Parnas, R. S., Hoes, K., and Sol, H., "Modelling of permeability of textile reinforcements: Lattice Boltzmann method", Composites Science and Technology, vol. 64, pp. 1069-1080, 2004.

[10] Verleye, B., Lomov, S. V., Long, A., Verpoest, I., and Roose, D., "Permeability prediction for the meso-macro coupling in the simulation of the impregnation stage of Resin Transfer Moulding", Composites Part A: Applied Science and Manufacturing, vol. 41, pp. 29-35, 2010.

[11] Verleye, B., Croce, R., Griebel, M., Klitz, M., Lomov, S. V., Morren, G., Sol, H., Verpoest, I., and Roose, D., "Permeability of textile reinforcements: Simulation, influence of shear and validation", Composites Science and Technology, vol. 68, pp. 2804-2810, 2008.

[12] Chen, Z.-R., Ye, L., and Lu, M., "Permeability predictions for woven fabric preforms", Journal of Composite Materials, vol. 44, pp. 1569-1586, 2010.

[13] Sharma, S. and Siginer, D. A., "Permeability measurement methods in porous media of fiber reinforced composites", Applied Mechanics Review, vol. 63, p. 020802 (19 pp.), 2010.

[14] Demaria, C., Ruiz, E., and Trochu, F., "In-plane anisotropic permeability characterization of deformed woven fabrics by unidirectional injection. Part I: Experimental results", Polymer Composites, vol. 28, pp. 797-811, December 2007 2007.

[15] Kuentzer, N., Simacek, P., Advani, S. G., and Walsh, S., "Permeability characterization of dual scale fibrous porous media", Composites Part A: Applied Science and Manufacturing, vol. 37, pp. 2057-2068, 2006.

[16] Okonkwo, K., Simacek, P., Advani, S. G., and Parnas, R. S., "Characterization of 3D fiber preform permeability tensor in radial flow using an inverse algorithm based on sensors and simulation", 2011.

[17] Adams, K. L., Miller, B., and Rebenfeld, L., "Forced in-plane flow of an epoxy resin in fibrous networks", Polymer Engineering and Science, vol. 26, pp. 1434-1441, 1986.

[18] Bickerton, S., Advani, S. G., Mohan, R. V., and Shires, D. R., "Experimental analysis and numerical modeling of flow channel effects in resin transfer molding", Polymer Composites, vol. 21, pp. 134-153, 2000.

[19] Parnas, R. S., Flynn, K. M., and Dal-Favero, M. E., "A permeability database for composites manufacturing", Polymer Composites, vol. 18, pp. 623-633, 1997.

[20] Lundström, T. S., Stenberg, R., Bergstrom, R., Partanen, H., and Birkeland, P. A., "In-plane permeability measurements: a nordic round-robin study", Composites Part A: Applied Science and Manufacturing, vol. 31, pp. 29-43, 2000.

[21] Arbter, R., Beraud, J. M., Binetruy, C., Bizet, L., Breard, J., Comas-Cardona, S., Demaria, C., Endruweit, A., Ermanni, P., Gommer, F., Hasanovic, S., Henrat, P., Klunker, F., Laine, B., Lavanchy, S., Lomov, S. V., Long, A., Michaud, V., Morren, G., Ruiz, E., Sol, H., Trochu, F., Verleye, B., Wietgrefe, M., Wu, W., and Ziegmann, G., "Experimental determination of the permeability of textiles: A benchmark exercise", 2011.

[22] Alms, J. B., Correia, N., Advani, S. G., and Ruiz, E., "Experimental procedures to run longitudinal injections to measure unsaturated permeability of LCM reinforcements", presented at the FPCM Collaboration, 2010.

[23] Alms, J. B., Correia, N., Advani, S. G., Ruiz, E., and Gonçalves, C. T., "Experimental procedures to run longitudinal injections to measure unsaturated permeability of LCM reinforcements", 2010.

[24] Sung Hoon, A., Woo Il, L., and Springer, G. S., "Measurement of the three-dimensional permeability of fiber preforms using embedded fiber optic sensors", Journal of Composite Materials, vol. 29, pp. 714-33, 1995.

[25] Endruweit, A., McGregor, P., Long, A. C., and Johnson, M. S., "Influence of the fabric architecture on the variations in experimentally determined in-plane permeability values", Composites Science and Technology, vol. 66, pp. 1778-1792, 2006.

[26] Luthy, T., "Three-dimensional permeability measurements based on direct current and ultrasound monitoring techniques", Ph. D. thesis, Physic, ETH, Neuchatel, 2003.

[27] Luo, Y., Verpoest, I., Hoes, K., Vanheule, M., Sol, H., and Cardon, A., "Permeability measurement of textile reinforcements with several test fluids", Composites - Part A: Applied Science and Manufacturing, vol. 32, pp. 1497-1504, 2001.

[28] Ferland, P., Guittard, D., and Trochu, F., "Concurrent methods for permeability measurement in resin transfer molding", Polymer Composites, vol. 17, pp. 149-158, 1996.

[29] Cao, J., Akkerman, R., Boisse, P., Chen, J., Cheng, H. S., de Graaf, E. F., Gorczyca, J. L., Harrison, P., Hivet, G., Launay, J., Lee, W., Liu, L., Lomov, S. V., Long, A., de Luycker, E., Morestin, F., Padvoiskis, J., Peng, X. Q., Sherwood, J., Stoilova, T., Tao, X. M., Verpoest, I., Willems, A., Wiggers, J., Yu, T. X., and Zhu, B., "Characterization of mechanical behavior of woven fabrics: experimental methods and benchmark results", Composites Part A: Applied Science and Manufacturing, vol. 39, pp. 1037-53, 2008.

[30] Lomov, S. V., Willems, A., Verpoest, I., Zhu, Y., Barburski, M., and Stoilova, T., "Picture frame test of woven composite reinforcements with a full-field strain registration", Textile Research Journal, vol. 76, pp. 243-52, 2006.